UNIVERSITY OF CAPE TOWN

PRODUCTION OF MID-CHAIN BRANCHED DETERGENT-RANGE OLEFINS OVER SHAPE-SELECTIVE ACID CATALYSTS

BY

MMONTSHI LEBOHANG OLIVER SUMANI

BSc (Chem.) (Cape Town), BSc (Chem. Hons) (Rhodes)

A thesis submitted to the University of Cape Town in partial fulfilment of the requirements for the degree of **Master of Science in Applied Science**

2006

SYNOPSIS

For the purpose of producing mid-chain mono-methyl branched olefins, a range of acid catalysts (MFI, BEA, TON and amorphous silica-alumina) were screened for the dimerization of 1-hexene, under generally mild conditions, viz. 150 – 170^{o}C, 20 - 40 bar and 1 – 4h^{-1} WHSV. It was postulated that shape-selective catalysts with defined pore sizes might improve selectivity towards mid-chain mono-methyl branched olefins. Such olefins are potential feedstocks for selectively branched detergents which have improved surfactant properties while retaining good biodegradability.

NMR and GC-MS analyses of hydrogenated dimer product fractions indicated that all catalysts produce branched products, and that these products are predominantly multi-branched (i.e. with two or more branches per C_{12} molecule). Overall, the findings of this study suggest a similar degree of branching of two for all catalysts.

Selective poisoning of the external surface of the MFI-90 catalyst using bulky bases effectively eliminated the catalytic activity, suggesting that in the case of MFI zeolite, the hexene dimerization reaction occurs largely (if not exclusively) on the external crystal surfaces which are not shape-selective.

In conclusion, BEA and amorphous silica-alumina pore being too large to induce shape selectivity and MFI and TON dimerization being limited to the external, non-selective, surface sites, the production of mono-methyl branched 1-hexene dimers was not accomplished.

ACKNOWLEDGEMENTS

First I would like to begin by thanking Sasol for the financial support and the opportunity they provided to me. From the Sasol's side I feel the following names have to be mentioned; P. Gibson and Dr. J.M Botha for letting me have this study leave, Dr C.P. Nicolaides for the project proposal, Dr M.N Kwini for her moral support and Dr. C.M Dwyer for proof reading my work. I would also like to extend my gratitude to the staff of the department of chemical engineering at UCT and in particular Prof. J.C.Q. Fletcher for his invaluable guidance during this period. M. Kirk and Dr. R. Bekker , thank you for the NMR analysis, this work would not be finished without you.

It will be injustice to conclude my acknowledgements without thanking my wife Grace for always being on my side during those trying periods I experienced, my colleagues at work for helping me to stay focussed, my family and, in closing, God.

TABLE OF CONTENTS

LIST OF SCHEMES

LIST OF FIGURES

LIST OF TABLES

LIST OF SYMBOLS

Symbol	Description	Units
X	conversion of 1-hexene	wt/wt
Y	mass yield of dimers	wt/wt
S	mass selectivity to dimers	wt/wt
F	mass flowrate	g/min
A	area under the chromatographic peak	-

GLOSARY

GC	Gas chromatography
NMR	Nuclear magnetic resonance
GASPE	Gated spin echo
GC-MS	Gas chromatography with mass spectrometric detector
GC-FID	Gas chromatography with flame ionic detector
WHSV	Weight hourly space velocity
TOS	Time-on-stream
HM	Heating mantle
THM	Thermometer
CNDS	Condenser
PI	Pressure indicator
TV	Two-way valve
RB	Round bottomed flask
W	Water
PS	Pressure sensor
CT	Cold trap
OV	one-way valve
EC	Electrical conductor
VP	Vacuum pump
LTA	Linde type A
FAU	Zeolite Y, feujasite
BEA	Zeolite beta
FER	Ferrierite
MWW	MCM-22
MAZ	Zeolite omega
MFI	MFI
MTW	ZSM-12
MTT	ZSM-23

1 INTRODUCTION

Fatty alcohols are aliphatic alcohols with chain lengths between C_6 and C_{22} and are represented by the general formula:

$$CH_3(CH_2)_nCH_2OH, \text{ where } n = 4 - 20$$

They are predominantly linear and monohydric, and can be saturated or have one or more double bonds. Alcohols with a carbon chain length above C_{22} are referred to as waxy alcohols. Diols whose chain length exceeds C_8 are regarded as substituted fatty alcohols. The character of the fatty alcohol (primary or secondary, linear or branched-chain, saturated or unsaturated) is determined by the manufacturing process and the raw materials used (Noweck, 2002).

Natural products, such as fats, oils, and waxes, and the Ziegler alcohol process provide linear, even-numbered, primary alcohols; those obtained from natural sources may be unsaturated. In contrast, the oxo process yields 20 – 60 % branched fatty alcohols and also some odd-numbered ones. Depending on the raw materials used, fatty alcohols are classified as natural or synthetic. Natural fatty alcohols are based on renewable resources such as fats, oils and waxes of plant or animal origin, whereas synthetic fatty alcohols are produced from petrochemicals such as olefins and paraffins.

Until 1930, when catalytic high-pressure hydrogenation was developed, the manufacture of fatty alcohols was based almost exclusively on the splitting of sperm whale oil. By 1962, the world capacity from natural raw materials had grown to ca. 200 000 t/a. New processes, utilizing petrochemical raw materials, e.g., the Ziegler, SHOP and oxo alcohol

processes, and the construction of additional plants for high-pressure hydrogenation of natural raw materials, further extended global production to some 2×10^6 t/a by 1999, roughly equally based on natural and petrochemical feedstocks. Fatty alcohols and their derivatives are used in polymers, surfactants, oil additives and cosmetics, and have many other specialty uses (Noweck, 2002).

Fatty chemicals obtained from natural sources have chain lengths of C_{16} – C_{18}. The limited availability of compounds with 12 – 14 carbon atoms, which are important in the production of surfactants, was one of the driving forces behind the development of petrochemical processes as well as the intensification of plantation and the breeding of new crops for the production of fatty alcohols. Other petrochemical processes have recently been developed for the synthesis of fatty alcohols from crude oil and coal derived feedstock. Commercial surfactants have chain lengths in the range of C_{12} - C_{18}.

The amphiphilic character of fatty alcohols, which results from the combination of a nonpolar, lipophilic carbon chain with a polar, hydrophilic hydroxyl group, confers surface activity upon these compounds. 70 – 75 % of fatty alcohol production is used in the manufacture of surfactants of various types, viz. anionic, cationic, amphoteric and non-inonic (Noweck, 2002). Surfactants are surface-active agents that, due to their physical and chemical characteristics, unfasten and remove dirt, and keep dirt and fat dissolved in the aqueous phase. They are present in many cleaning products such as laundry detergents, household washing detergents, shampoos and hair conditioners.

Changes in legislation demanding products with improved environmental biodegradability as well as customer requirements for lower wash

temperatures, a growing need to find alcohol intermediates which are both biodegradable and show good detergency at cold wash temperatures, is to be expected. It has been reported that mid-chain branched fatty alcohol-based surfactants indeed exhibit such characteristics (Blain et al., 1991, Cripe et al., 1999, Giacobbe and Ksenic., 1992, 1993, Jensen and Culver, 2001, Page et al., 1989, Singleton et al., 1998a, 1998b, 2001, Vinson et al., 2000). These claims, coupled with a globally increasing supply of 1-hexene (Houston, 1998), suggest that the production of suitable detergent-range intermediates and products may be achieved via 1-hexene dimerization to C_{12} olefins followed by hydroformylation and hydrogenation to the desired alcohols.

As a consequence, this study seeks to evaluate the performance zeolite catalysts for the dimerization of 1-hexene to mid-branched C_{12} detergent olefins.

2 BACKGROUND

2.1 Detergency and biodegradability

As a general term, detergency means cleaning power (Rosen, 1989). However, when applied to a surface-active agent, detergency refers to its special property for enhancing the cleaning power of a liquid. This is accomplished by a combination of effects involving adsorption at interfaces, alteration of interfacial tensions, solubilization, emulsification, and the formation and dissipation of surface charges.

In general, cleaning consists essentially of two processes, viz. removal of the soil (material to be removed from the substrate in the cleaning process), and the suspension of the soil in the bath and prevention of redeposition. This second process is as important as the first since it prevents redeposition of the soil onto another part of the substrate (Rosen, 1989).

There is a relationship between the chemical structure of the surfactant and its detergency. These correlations are complicated by the differing soils and substrates to be cleaned, by the amount and nature of builders present, by the temperature and hardness of the water used in the bath, and by the different mechanisms by which soils are removed. Correlations are therefore valid only when many of these variables are specified and controlled.

An example is as follows: to achieve optimum oil soil (dirt from fatty substances) removal, the required chain length of the hydrophobic group in nonionic surfactants decreases as the wash temperature decreases (Rosen, 1989). Thus for nonionic surfactants having similar cloud points, the order of maximum oil soil removal from polyester/cotton is as follows:

at 70°C: $C_{14} = C_{12} > C_{10}$,

at 38°C: $C_{10} = C_{12} > C_{14}$,

at 24°C: $C_{10} > C_{12} > C_{14}$.

Nonionics have also been shown to be more effective than ionics in the removal of oily soil from relatively nonpolar substrates (Rosen, 1989).

The need for waste water reuse has prompted governments throughout the world to enforce the requirement for biodegradable surfactants. Biodegradation of surfactants or other organic components is primarily achieved by bacterial action. In this degradation, the organic molecule passes through many intermediate stages before complete conversion to CO_2 and H_2O. It is generally accepted that the chemical nature of the hydrophilic group affects biodegradability to a minor extent while that of the hydrophobic group plays the dominant role (Stache, 1996). The relationship between chain length, the degree of branching and the position of attachment to the hydrophobe, respectively, and biodegradability is complex as described below.

Huddleston and Allred (Schick, 1999) have investigated the effect of the hydrophobic group structure on the biodegradability of various polyoxyethylene alkylphenols. The data obtained showed the degradation of polyoxyethylene straight chain alkylphenols to increase with increasing chain length of the alkyl chain. Furthermore, the bioresistance of polyoxyethylene branched-chain nonylphenol exceeded that observed for the corresponding straight-chain compound (Schick, 1999).

The findings of a study by Blankenship and Piccoli (Schick, 1999) on the degradation of a series of polyoxyethylene fatty alcohols with differing hydrocarbon chain lengths i.e. from C_{10} to C_{16}, containing equal weight fractions of ethylene oxide are presented in Figure 2.1.

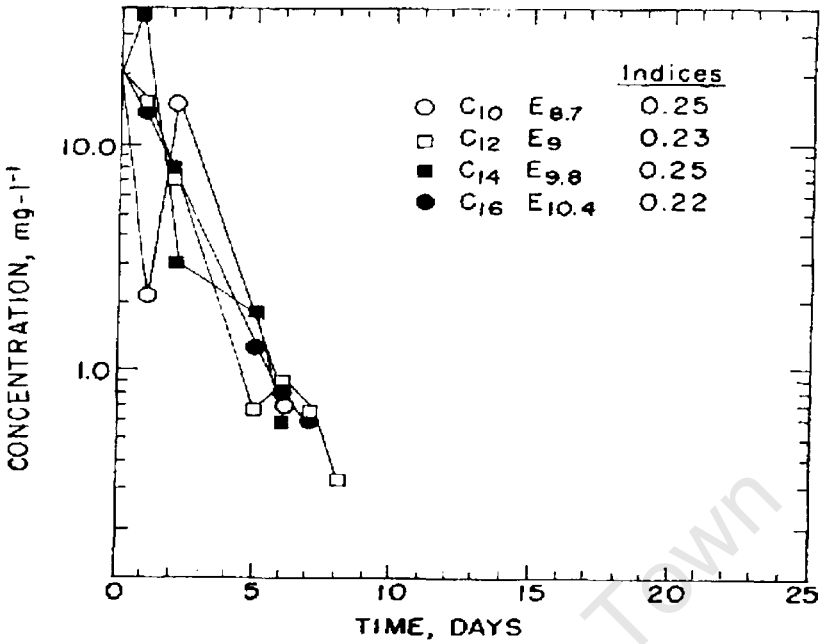

Figure 2.1: Variation in rate of degradation with hydrophobic chain length (Schick, 1999).

Within experimental accuracy, all compounds seem to degrade at about the same rate. From these and other studies of anionic surfactants, a basic principle becomes evident, viz. straight-chain hydrophobes are more readily biodegradable than branched chains. The same principle holds true for all types of nonionic surfactants (Schick, 1999). However, it has also been observed (Stache, 1996) that when the alcohol based surfactant is singly branched, biodegradability is very similar to that of linear alcohols. In contrast, highly branched alcohols, such as isotridecyl alcohols and alkylphenols, markedly retard the ultimate biodegradability. Battersby et al. (2000) performed studies to determine the effect of quaternary carbons on biodegradability of alcohol-based surfactants (Figures 2.2 and 2.3). In their studies, compounds were tested for biodegradation. From Figure 2.2, it is clear that although biodegradation of a C_{15} alcohol sulphate containing vicinal methyl groups was slower than sulphated C_{14}/C_{15} SHF (Shell hydroformylation) alcohols (linear fraction and 80/20% linear to branched mixture), biodegradation still easily exceeded the pass level for 'ready'

biodegradability by Day 28. In contrast, the quaternary C_{15} alcohol sulphate showed no biodegradation over the test period. As the latter compound contains multiple branching in addition to a quaternary carbon, and in order to test the possibility that multi-branching was the primary factor inhibiting biodegradation (versus the presence of quaternary carbon), the authors synthesised the model C_{15} alcohol 3,7,11-trimethyl dodecanol and tested it as a sulphate for biodegradability. This compound contained multiple branching but not a quaternary carbon. It can be seen from Figure 2.3 that the biodegradation of 3,7,11-trimethyl dodecanol sulphate was similar to that of $C_{14}/_{15}$ SHF alcohol sulphate. In contrast, the quaternary C_{15} alcohol sulphate was again not biodegradable.

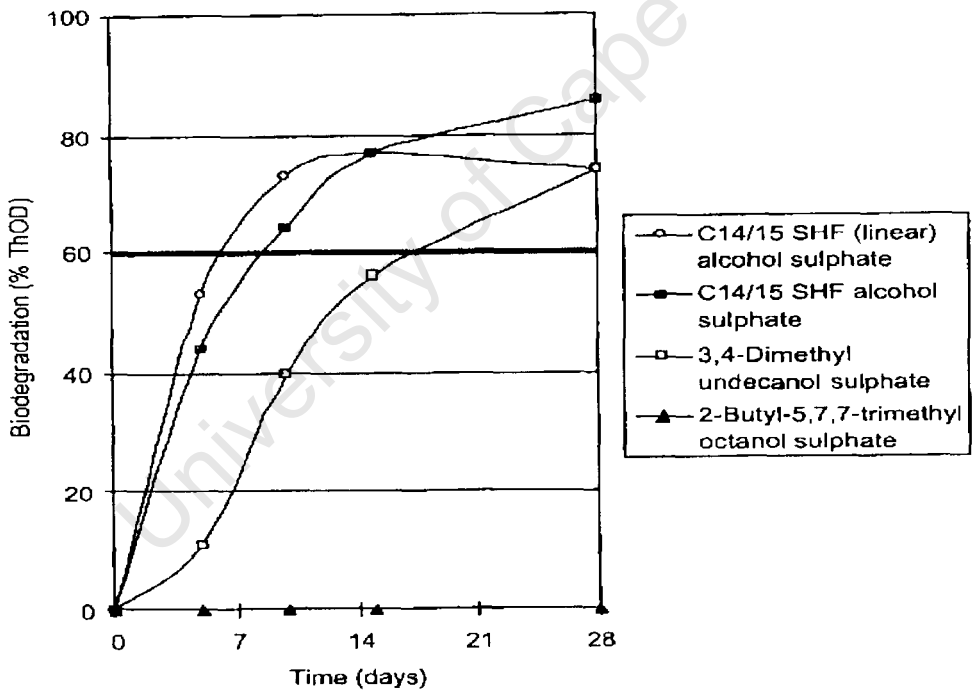

Figure 2.2: Biodegradation of model alcohol sulphates containing vicinal methyl groups or a quaternary carbon (Battersby et al., 2000). [ThOD = Theoretical Oxygen Demand.]

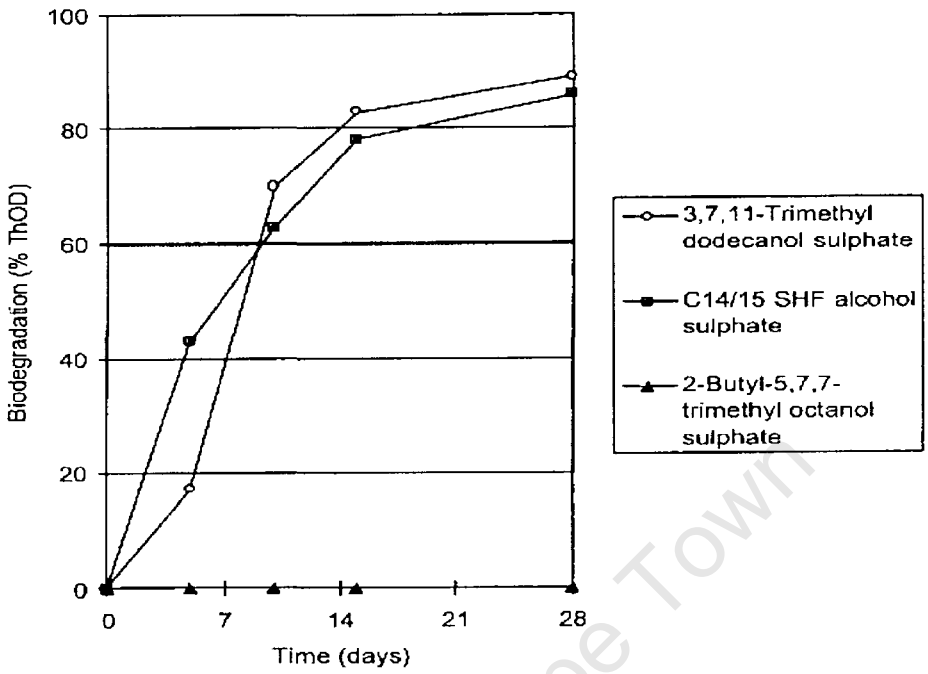

Figure 2.3: Biodegradation of model alcohol sulphates containing either multiple branching or a quaternary carbon (Battersby et al., 2000). [ThOD = Theoretical Oxygen Demand.]

Smithson (Schick, 1999) studied the effect of the position of the attachment to the hydrophobe on the biodegradation of polyoxyethylene straight-chain alkylphenol precursors of sulphated derivatives. It is reported that optimum biodegradability was obtained when the phenol was attached close to the end of linear alkyl chain. Thus, the o-2-isomer is more readily degradable as evidenced from data of Table 2.1.

Table 2.1: Effect of phenyl attachment on biodegradability of linear polyoxyethylene nonylphenol suphates (Schick, 1999).

	Percent degraded	
	Mild	Strong
o-2-Nonylphenol	90	>90
o-5-Nonylphenol	0	0

These results indicate the following;

- There is no significant difference between singly branched and linear surfactants as far as the biodegradability is concerned.
- C_{12} surfactants exhibit good detergency throughout the temperature range of practical interest.
- The position of the alkyl group branch is preferably towards the centre of hydrocarbon chain.
- A further increase in the degree of branching, beyond singly branched, is accompanied by a decrease in biodegradability.
- The presence of quaternary carbons in a surfactant molecule severely deteriorates biodegradability.

The implication of these findings is that mid-branched C_{12} surfactants are likely to exhibit excellent performance in terms of both biodegradability and detergency across a wide range of wash temperatures, including good cold water detergency.

2.2 Industrial practice

Typical, commercially available long chain alcohols are the NEODOL® alcohols (oxo products) made by Shell and the EXXAL® alcohols produced by ExxonMobil and the SAFOL® products produced by Sasol. The highly linear NEODOL® derived products are commercially successful in part because of their high linearity which renders them readily biodegradable (Singleton et al., 1998a). However, their linearity also imparts significant hydrophobicity to the hydrocarbon chain, thereby decreasing its cold water solubility and detergency. In contrast, the EXXAL® 13 product, which is derived from propylene oligomerization, is highly branched and therefore poorly biodegradable. However, the EXXAL® 13 products ensure high cold water detergency (Singleton et al., 1998a).

2.2.1 Homogeneous catalytic systems for detergent-range olefins

2.2.1.1 Shell process using nickel catalysts

A process for the production of "mono-branched alcohols", via olefin dimerization, wherein the average number of branches per product molecule ranges from 0.9 to 2.0, has been reported by Shell (Singleton et al., 1998b, 2001). The homogeneous catalyst employed comprises a mixture of a nickel carboxylate or a chelated nickel complex, in conjunction with an alkyl aluminium halide or an alkyl aluminium alkoxide, and is applicable for the dimerization of C_6 - C_{10} olefins. The resulting detergent–range olefins show branching principally towards the centre of the hydrocarbon chain, with side chain lengths varying from 1 to 4 carbon atoms with decreasing propensity. Thus, dimerization of lower olefins using a homogeneous nickel catalyst produces mid-branched detergent–range alcohols (Singleton et al., 1998b, 2001). The proposed dimerization reaction mechanism over the nickel catalyst is given, for the example of 1-hexene, in Scheme 2.1 (O'Connor, 1990, Skupiñska, 1991).

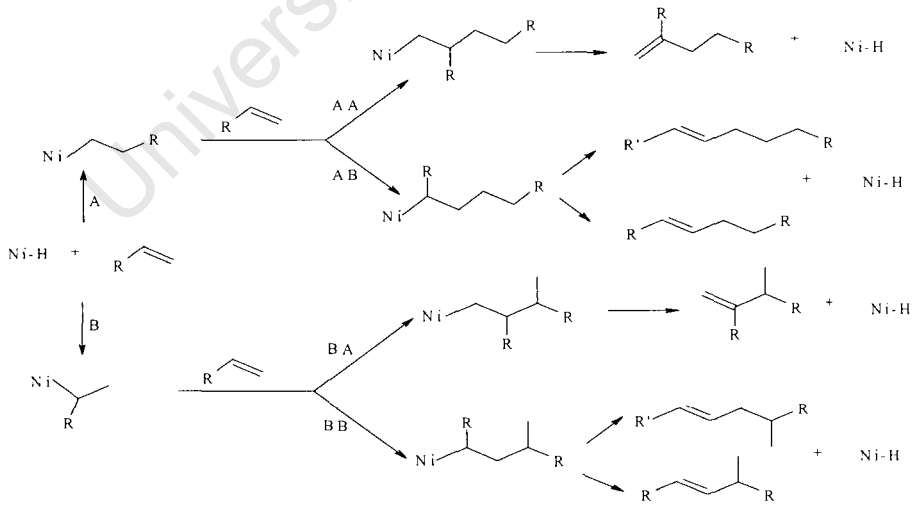

Scheme: 2.1: Mechanism of 1-hexene dimerization in the presence of a nickel complex (A = Addition of the olefin primary carbon to the nickel atom, B = addition of the olefin secondary carbon to the nickel atom, R = C_4 and R' = C_3).

The non-selective nature of the catalytic system in terms of the position of the olefin insertion suggests, however, that it might be difficult to control the oligomerization reaction towards desired oligomers, i.e. both branched (paths AA, BA and BB in scheme 2.1) or linear (path AB in scheme 2.1) dimers will be produced. Nonetheless, from a comparison of the results reported in the Shell patents (Singleton et al., 1998b, 2001) and the findings of others including Skupińska (1991) and Keim et al. (1979), it can be concluded that homogeneous nickel catalyst systems may be tailored to yield either predominantly branched or predominantly linear products, depending on the nickel ligand and/or the reaction conditions.

2.2.1.2 The Procter and Gamble process

The Procter and Gamble process for the preparation of the mid-chain branched fatty alcohols is presented in scheme 2.2 (Cripe et al., 1999, Vinson et al., 2000, Jensen and Culver, 2001).

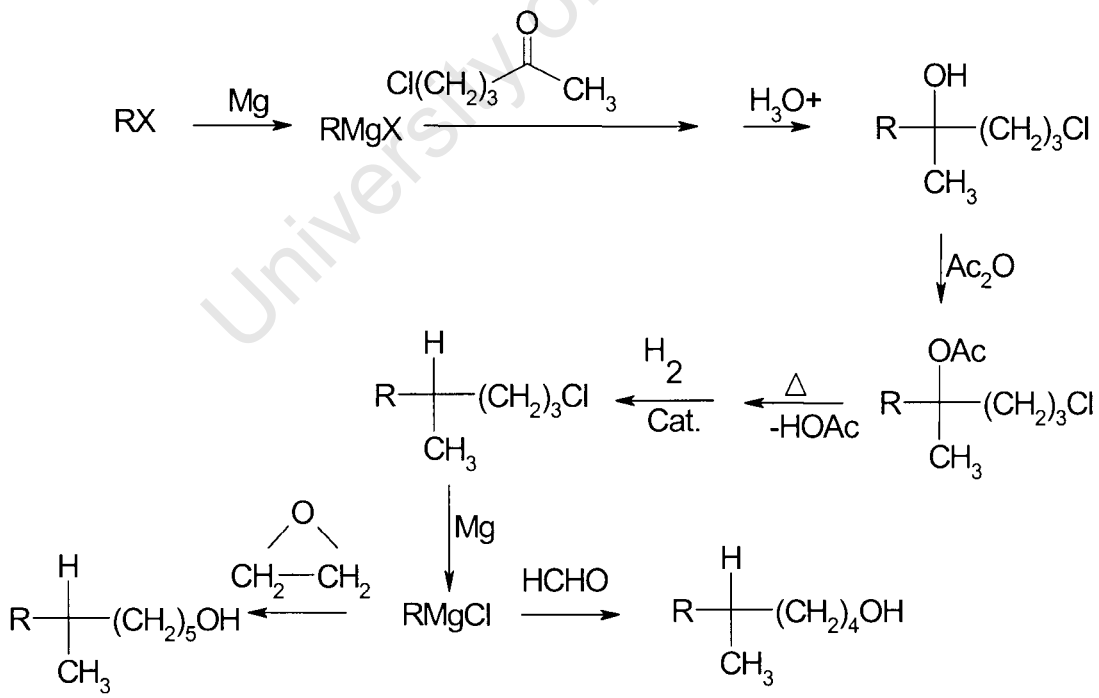

Scheme: 2.2: Preparation of the mid-chain branched fatty alcohols as produced by Procter and Gamble.

In this process, an alkyl halide is converted to a Grignard reagent followed by reaction with a haloketone. After conventional acid hydrolysis, acetylation and thermal elimination of acetic acid, an intermediate olefin is produced which is subsequently hydrogenated over catalysts such as Pd/C. Formylation of the alkyl halide resulting from the hydrogenation step affords the alcohol product. Further branching can, for example, be accomplished by reaction with ethylene oxide, as shown in Scheme 2.2. In terms of both mono- and di-branched mid-chain branched alcohols, typical products are presented in Figure 2.4.

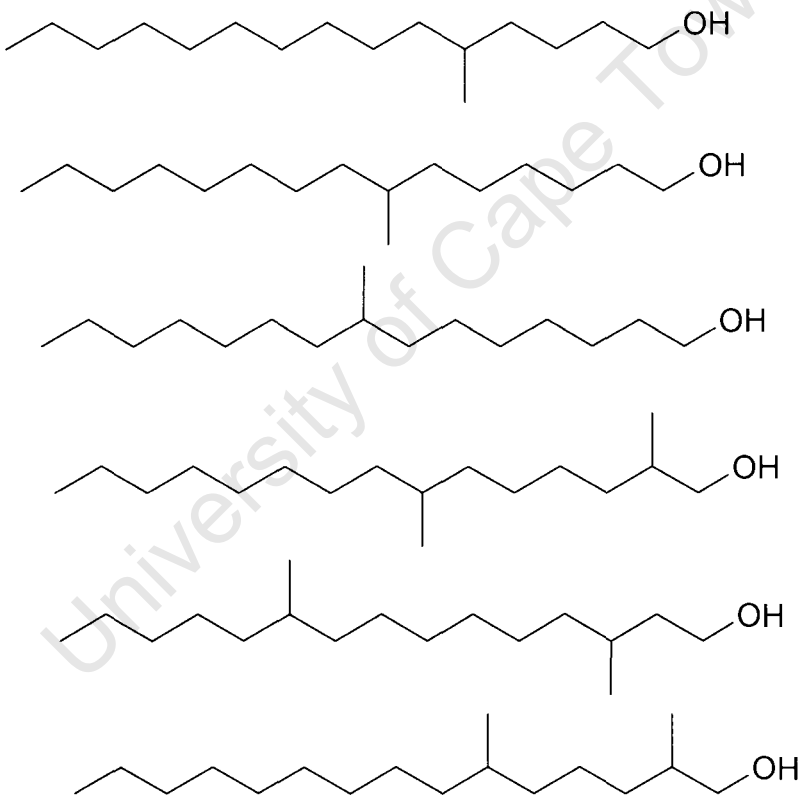

Figure 2.4: Typical alcohols produced via the Procter and Gamble process

Based on patent claims (Cripe et al., 1999, Jensen and Culver, 2001, Vinson et al., 2000), the performance of the surfactants so obtained is comparable to those obtained via the Shell process (Singleton et al., 1998b, 2001).

2.2.2 Heterogeneous catalytic systems for detergent-range olefins

2.2.2.1 Skeletal isomerisation of detergent-range olefins over solid acid catalysts

A heterogeneous process for the production of mid-chain branched detergent-range olefins has been reported by Shell (Singleton et al., 1998a), in which a detergent range olefin (C_{12} - C_{17}) is isomerised over an acid catalyst (FER) to the corresponding skeletal isomers..After hydroformylation, the intermediate alcohol products have an average of 1.3 – 1.6 branches per chain. Moreover, mid-chain branching is favoured as are shorter side chain lengths. No quaternary carbon atoms were detected. It was further shown that these branched compounds are readily biodegradable and exhibit improved cold and warm water detergency in comparison to sulfated NEODOL® linear alcohols of equivalent carbon chain length (Giacobbe and Ksenic, 1992, Singleton et al., 1998a, 1998b, 2001).

2.2.2.2 Shape-selective acid-catalysed oligomerization of lower olefins to detergent-range olefins

Patents assigned to Mobil Oil Corporation report the oligomerization of C_3 and C_4 olefins over a surface-deactivated, shape-selective MTT zeolite catalyst (Blain et al., 1991, Giacobbe and Ksenic, 1992, 1993, Page et al., 1989). Structural properties of the products of propylene oligomerization at 200 ºC, 35 bar and WHSV of 0.22 hr^{-1} are summarised in Table 2.2.

Table 2.2: Structural properties of products obtained from propylene oligomerization over surface deactivated MTT (Page et al., 1989).

TOS[a](days)	1	2	3
C_9 products			
>=Di-Me[b]	7.30	5.50	5.80
Mono-Me[c]	62.0	65.8	68.0
Normal	30.6	28.8	26.2
Average branches per molecule	**0.80**	**0.80**	**0.82**
C_{12} products			
> or = Di-Me	9.70	10.3	10.3
Mono-Me	69.9	74.1	75.2
Normal	20.3	15.6	14.5
Average branches per molecule	**0.94**	**1.00**	**1.01**
C_{15} products			
>=Di-Me	12.5	13.5	14.4
Mono-Me	73.4	77.3	78.3
Normal	14.2	9.20	7.20
Average branches per molecule	**1.05**	**1.11**	**1.14**

[a]TOS = time-on-stream, [b]>= Di-Me = olefins having two or more methyl side chains, [c]Mono-Me = olefins with one methyl side chain.

In the absence of external surface deactivation the same catalyst (MTT; 200°C, 35 bar and WHSV of 0.50 hr^{-1}) produced an average branching per C_{15} molecule of 3.8, which is substantially larger than that obtained over the surface deactivated catalyst (see Table 2.2). Similar results were obtained for butylene oligomerization (Page et al., 1989), clearly demonstrating the shape selective nature of the surface-deactivated MTT to limit the branching to methyl groups and especially to mono-methyl branching (> 60% selectivity). Most significantly, the number of branches may be limited to approximately one per 15 carbon atoms in the chain. Moreover, the alcohol-based surfactants derived from this process were reported to be both biodegradable and to exhibit improved low temperature detergency.

2.3 Experimental literature

2.3.1 Oligomerization of olefins over zeolites and molecular sieves

Quann et al. (1988) investigated the oligomerization of propylene over MFI, demonstrating a substantial reduction in branching as compared with the branching expected for an unconstrained acid catalyst (Figure 2.5). This finding was ascribed to the shape selective properties of the MFI structure.

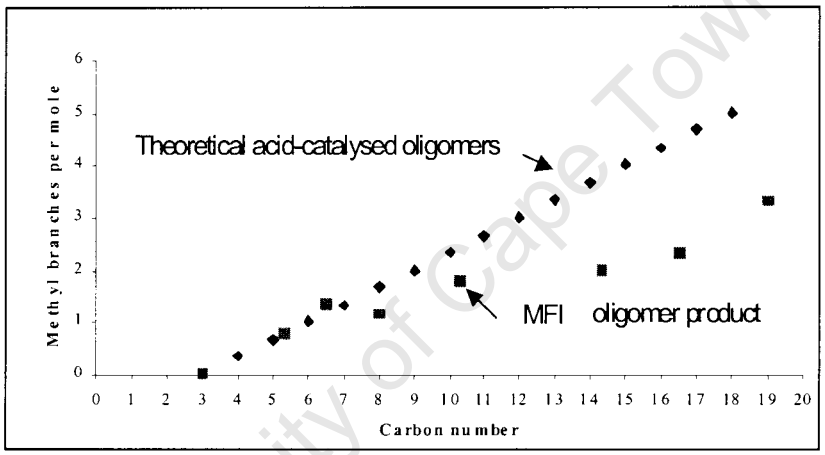

Figure 2.5: Methyl branching in propylene oligomers obtained over MFI versus that expected over a non shape-selective acid catalyst (Quann et al., 1988).

Similarly, Pater et al. (1999) evaluated a series of catalysts including MWW zeolite for the oligomerization of 1-hexene. Mainly dimers were formed, with the following product selectivities: mono-branched < 20%, di-branched > 65% and tri-branched < 25%, for all the catalysts tested. Thus, mono- and di-branched dimers constituted the majority of the product and, in the case of the di-branched dimers, the two branches are on adjacent carbons as would

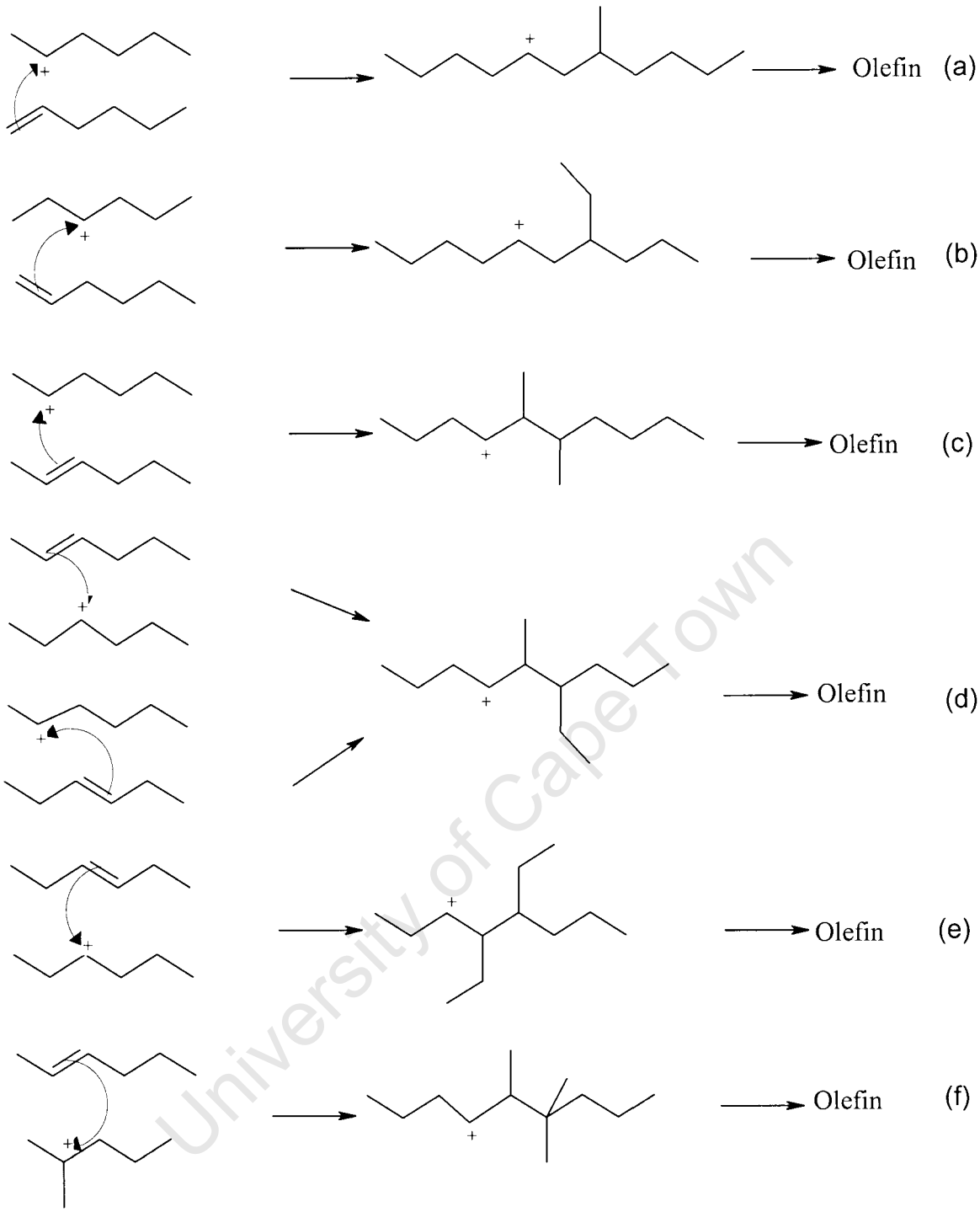

Scheme 2.3: Examples of hexene dimerization reactions leading to the formation of mono-, di- and tri-branched C_{12} olefins over acid catalysts (Pater et al., 1999).

be expected from the mechanism of the acid-catalysed dimerization reaction (as represented in Scheme 2.3)

Although little is reported on the type of branching (methyl, ethyl etc.) or on any shape-selective properties, it is reasonable to expect that the formation of highly branched products (such as [d] and [e] in Scheme 2.3) is limited in medium pore zeolites. It should be noted, however, that several authors observe only limited shape selectivity in the product of 1-hexene oligomerization at low temperatures (50 – 300°C) (Anderson et al., 1989, Pater et al., 1999, Quann et al., 1988), which has been ascribed to coking and subsequent pore blockage with the dimerization reaction being catalysed predominantly by the external surface. Based on these findings, it may be necessary to optimise reaction conditions to avoid intraparticle coking in order to take advantage of molecular sieve or zeolite shape-selectivity.

2.3.2 Other catalytic systems for olefin oligomerization

Table 2.3, summarises the results of several studies of olefin oligomerization, mainly for 1-hexene monomer but other monomers are also included (where 1-hexene data is unavailable).

2.3.2.1 Titanium and zirconium

Titanium and zirconium catalysts are known to be effective for the oligomerization and polymerisation of higher α-olefins. As a consequence of their high activity, these catalytic systems are not suitable for the selective dimerization of 1-hexene since they favour polymerisation. The products obtained in these catalytic systems are reported to be highly branched (Skupiñska, 1991).

2.3.2.2 Lewis acid type catalysts ($AlCl_3$ and BF_3 systems)

$AlCl_3$ and BF_3 are effective catalysts for higher α-olefin oligomerization in the presence of a proton donating co-catalyst (Skupiñska, 1991), and

Table 2.3: Oligomerization of higher α-olefins (Skupińska, 1991).

Catalyst	Olefin/react condtn	Selectivity to Products (%)	Conversion (%)
HOMOGENEOUS SYSTEMS			
	titanium		
$TiCl_4$/propylene oxide/$(C_2H_5)_3Al_2Cl_3$ (Al/Ti = 1.25).	1-octene/hexene	C_{24} = 65	80
	zirconium		
$ZrCl_4(HfCl_3)/AlCl_3$ Al/Zr = 1	1-decene/heptane, 99°C, 1h	C_{30-50} = 50	93
	tungsten		
$WCl_3/LiAlH_4$	1-hexene/chlorebenzene, 25°C, 75 min.	Branched oligomers (Distribution not shown)	100
	aluminium		
$C_2H_6AlCl_2$/RCl (1:1.5-2)	1-hexene/20°C, 90min, heptane/hexene = 1:1	Highly-branched oligomers (Distribution not given)	100
AlX_3 or $RAlX_2$/ haloalkanoic acid, X = Cl, F	1-hexene/nonpolar solvent, 70°C, 24h	C_{12} = 20 C_{18} = 40 C_{24} = 10	95
	BF_3 system		
BF_3(gas)/$BF_3.2H_2O$	1-hexene, 20 -50°C	C_{12} = 1.8 C_{18} = 68.4 $C_{>24}$ = 29	99
	nickel based systems		
$Ni(HCOO)_2$/ $(C_2H_5)_3Al$ (Al/Ni=40)	1-hexene/toluene, 60°C, 4h	∝-olefins = 89	38.3
$Ni(acac)_2/(C_2H_5)_3Al_2Cl_3/Ph_3P$	1-hexene/toluene, 60°C, 4h	∝-olefins = 50	63
HETEROGENEOUS SYSTEMS			
	non-zeolite acid catalysts		

Table 2.3 continued

Catalyst	Olefin/react condtn	Selectivity to Products (%)	Conversion (%)
5% $Cr/Al_2O_3/SiO_2$	1-hexene,	(Distribution not reported)	Not reported
$TaCl_6/SiO_2$	1-hexene/100psig, 100°C	C_{12} = 70%	60
		C_{18} = 14%	
	zeolites	$C_{>24}$ = 17%	
MFI zeolite	1-hexene/359-593K	C_{12} = max + other byproducts	Not reported
MTW zeolite	1-pentene/200-400psig, 392-482°F	97% C_{10} C_{12-18} oligomers	76

yield branched products.

2.3.2.3 *Heterogeneous nickel catalyst systems*

Nickel (II)-exchanged silica-alumina is active for olefin oligomerization (Nicolaides and Scurrell, 2001) and such nickel-based systems show high dimer selectivity. A comprehensive analysis of the resulting dimer fraction is presented in Table 2.4 from which it can be observed that internal olefins predominate. Although for the example of Table 2.4 linear and branched products occur in almost equal amounts, acidity associated with the aluminosilicate support may be adjusted so as to effect some control of the degree of branching.

Table 2.4: Dimer isomer distribution from propylene oligomerization at 110°C and 35 bar over ion-exchanged nickel on silica-alumina (Nicolaides and Scurrell, 2001).

Isomer	mass% in $C_6^=$	Relative mass% within each geometric isomer group	
		Experimental	Equilibrium*
1-Hexene	1.5	3.3	1.0
cis-3-Hexene	1.2	2.7	4.0
trans-3-Hexene	7.8	17.4	20.2
cis-2-Hexene	9.4	20.9	41.6
trans-2-Hexene	25.2	55.7	33.2
Total linear	45.1	100.0	100.0
4-Me-1-pentene	3.1	8.8	4.2
4-Me-*cis*-2-pentene	6.9	19.6	31.5
4-Me-*trans*-2-pentene	25.2	71.6	64.3
Total	35.2	100.0	100.0
2-Me-1-pentene	2.1	16.9	25.2
2-Me-2-pentene	10.3	83.1	74.8
Total	12.4	100.0	100.0
2,3-diMe-1-butylene	0.7	15.2	45.9
2,3-diMe-2-butylene	3.9	84.8	54.1
Total	4.6	100.0	100.0
Other products	2.7	n.a.	n.a

* Equilibrium distribution calculated from thermodynamic data.

2.3.2.4 *Supported phosphoric acid catalysis*

Best represented by the UOP "solid phosphoric acid" (SPA) catalysts, these systems produce highly branched products as a consequence of the carbenium ion mechanism, and are employed in the production of EXXAL® 13 olefin intermediates. Although a substantial improvement over liquid phosphoric acid systems, SPA catalysts remain corrosive (Skupińska, 1991) and generally have short lifetimes (3 – 9 months) due to pressure drop build-up caused by catalyst fouling in the multitubular reactor configuration in which they are applied.

2.3.3 Other reactions catalysed by zeolites during the oligomerization of olefins

The extent of oligomerization depends on both temperature and pressure. However, other acid catalysed reactions such as cracking, skeletal isomerisation, cyclisation and aromatisation also occur. The relative rates of these various acid-catalysed reactions are presented in Table 2.5.

Table 2.5: Relative rates of various reactions over MFI at 1 atmosphere and 450°C (Haag and Chen, 1987).

Reaction	Feed	Relative rate constants
Cracking	Hexene	1
	Nonane	3.2
	Dodecane	23
Isomerisation	*m*-Xylene	226
Polymerisation	Propylene	868
Cracking	1-Hexene	782
	1-Heptene	1209
Double-bond shift	1-Hexene	1×10^6

The extremely high relative rate constant for the double-bond shift reaction implies that an olefin will readily undergo double-bond isomerisation as the main side-reaction during the acid-catalysed oligomerization process. A consequence, although 1-olefin feed may be used, the reactive monomer will likely include all double bond isomers. For MFI catalysed 1-hexene oligomerization, Quann et al. (1988) found that double-bond isomerisation predominated at low conversions,

whereas both double-bond and skeletal isomerisation occurred at high conversions (Figure 2.6).

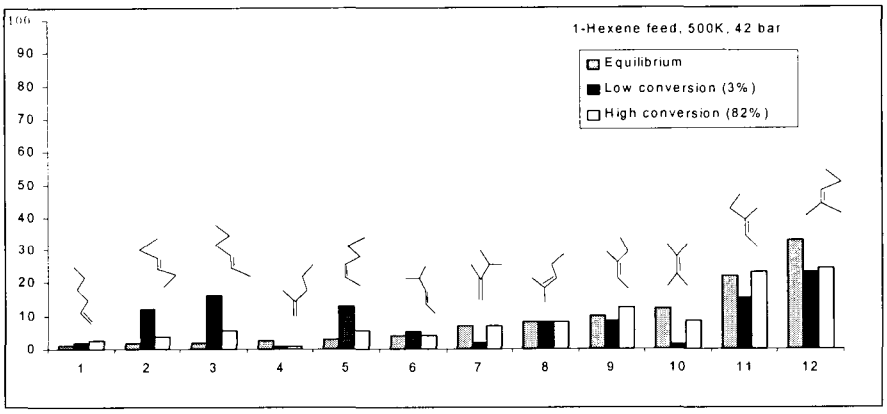

Figure 2.6: Hexene isomer distribution at low and high conversions over MFI and at equilibrium (Quann et al., 1988).

Pater et al. (1999) also observed the same reactivity towards the double bond-shift reaction for a range of catalysts that were screened for 1-hexene oligomerization and reported that 1-hexene rapidly isomerised to *cis*-and *trans*-2-hexenes. From both the equilibrium and experimentally observed isomer distributions (Figure 2.6), it is clear that if the skeletal isomerisation can be limited, the feed concentration will always be higher in 2-hexenes than in 1-hexene. In conclusion, therefore, temperature and pressure should be optimised in order to avoid side-reactions (such as skeletal isomerisation and cracking) and to promote the olefin oligomerization reaction.

2.3.4 Summary of reported findings

From this review, it is clear that several catalytic systems have been studied for the oligomerization of olefins. It is also clear that there are no known higher olefin oligomerization commercialised processes that are aimed at producing mid-chain branched olefins. However, reports of the successful production of predominantly mid-chain branched higher olefins from butylene oligomerization over MTT catalysts with external surface deactivation (Page et al., 1989) suggest that prospects for similar results may be achieved via 1-hexene dimerization.

2.4 Zeolite catalyzed oligomerization

Zeolites are among the most important acid catalysts used for the oligomerization of olefins. At higher reaction temperatures and conversions, a range of sequential and parallel reactions such as cracking, copolymerization and disproportionation leads to a continuous distribution of components with respect to carbon number in the product spectrum (O'Connor, 1997). These reactions are enhanced at higher olefin partial pressures and higher aluminium contents of zeolites. The olefin oligomerization reactions are therefore conducted at low temperatures in order to minimise side reactions.

The nature and number of acid sites play a key role in the catalytic performance of zeolites. However, in most instances, zeolite performance for olefin oligomerization is substantially influenced by pore geometry and size. The most common observation is that the large-pore zeolites allow for the formation of bulky polynuclear aromatics which lead to deactivation by coke formation and this deactivation may take place by pore mouth blockage. Small and medium pore zeolites are shape-selective to feed, transition-state intermediate/s and products depending on pore size and geometry, as illustrated by the fact that the degree of branching decreases as pore size decreases in the following order (average pore size in Å): MAZ (7.5) > FAU (7.4) > MOR (6.5 X 7) > MFI (5.3 X 5.6) (O'Connor, 1997).

The large pore zeolites such as MAZ and FAU also undergo rapid deactivation during these processes as a result of the ease of formation of the bulky polynuclear aromatic coke precursors. Moreover, a one dimensional pore structure is not suitable for the oligomerization reaction as a result of coking leading rapidly to pore mouth blockage, e.g. as in the case of zeolite MOR. ^{1}H-NMR studies have shown that the average number of carbon atoms between branches for propylene oligomerization over MFI is 4 as opposed to 2 over amorphous silica-alumina and 1 over phosphoric acid catalysts, respectively (O'Connor, 1997). These observations emphasize the importance of a proper zeolite catalyst choice for desired oligomer branching i.e. large pore for highly branched oligomers and vice versa.

2.5 Zeolite catalysts

Zeolites structures offer a rich diversity of channel (pore) sizes and shapes, channel dimensions and connectivities, and active site type and concentration. The size and morphology of their crystallites may also be varied.

2.5.1 Zeolite structure and acidity

2.5.1.1 Zeolite structural features

Small pore zeolites with 8-membered ring channels (e.g. LTA), typically sorb linear molecules such as n-paraffins or primary alcohols, but not branched isomers (Venuto, 1994). The structure of LTA is shown in Figure 2.7.

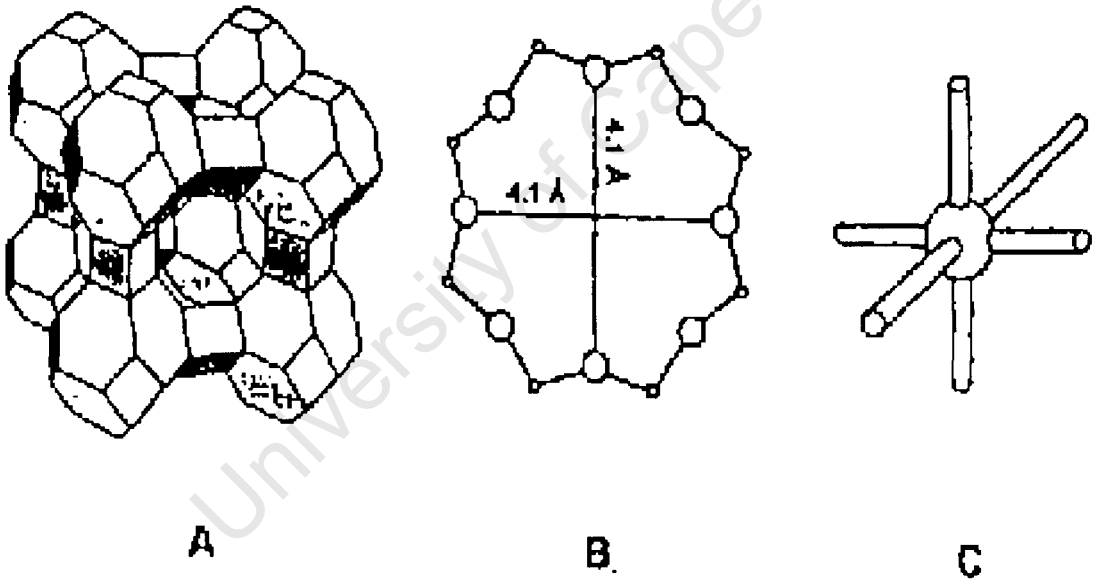

Figure 2.7: LTA structure. (A) Line drawing. (B) 8 – ring viewed along [100]. (C) Schematic representation of pore channel system in zeolite A (Venuto, 1994).

Medium-pore zeolites, comprising 10-membered rings, generally have more uniform channel (pore) dimensions. Large cages with restricted access via smaller windows such as in LTA and FAU are typically absent (Venuto, 1994). The intermediate size of their channels potentially enables a remarkable range of discrimination in molecular transport and chemical reaction. In MFI type zeolites (Figure 2.8), two

perpendicular intersecting 10-ring channel systems form a three-dimensional network. One channel is straight with near-circular (5.3 X 5.6 Å) openings, while the other is tortuous (sinusoidal or zig-zag) with elliptical openings (5.1 X 5.6 Å).

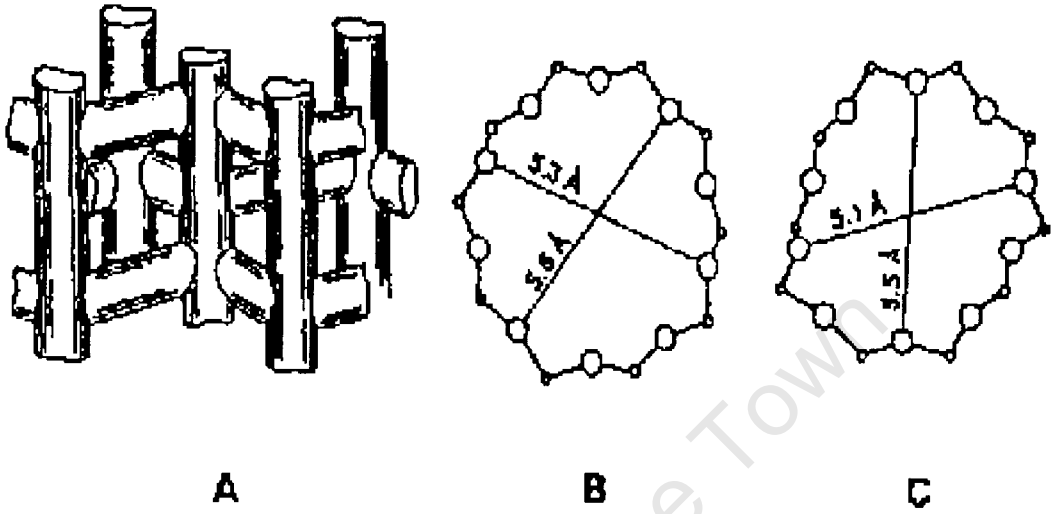

Figure 2.8: MFI structure. (A) Model showing intersecting straight and sinusoidal channels. (B) 10 – Ring from straight channel viewed along [010]. (C) 10 – Ring from sinusoidal channel viewed along [100] (Venuto, 1994).

The presence of 12-membered rings is a characteristic of the large-pore zeolites, with the obvious potential for sorption and conversion of large molecules e.g. FAU (Figure 2.9).

The FAU pore channel system is a very open, three-dimensional network with tetrahedral geometry containing a series of roughly spherical supercages (~11.4 Å diameter) connected by four tetrahedrally oriented 7.4 Å diameter (distorted 12-membered ring) windows. FAU has relatively low Si/Al ratios associated with potentially high cation-exchange capacity and active site density.

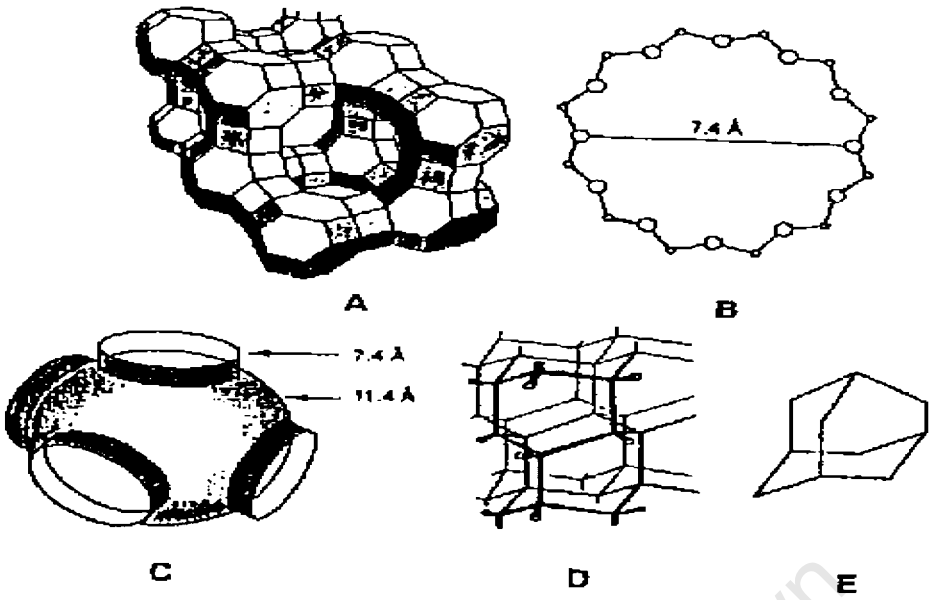

Figure 2.9: FAU structure. (A) Line drawing. (B) 12 – Ring viewed along [111]. (C) Visualization of FAU supercage (~11.4 Å diameter) with its four smaller (12 – ring) windows. (D) Adamantoid (tetrahedral) pore-channel system in FAU. (E) Structure of adamantine for reference (Venuto, 1994).

2.5.1.2 Zeolite acidity

Figure 2.10 shows the structure of the hydrogen or Brønsted acid form of a zeolite. Since each lattice AlO_4-tetrahedron is associated with unit negative charge, cations are required to maintain charge neutrality. Although the existence and importance of protonic acid sites in zeolite catalysis is now well established, they are by no means the only type of active sites in these microporous compositions. Lewis acid sites (Figure 2.11) may also be present but there are uncertainties with regard to the catalytic significance of these active centers for the oligomerization of olefins (Venuto, 1994).

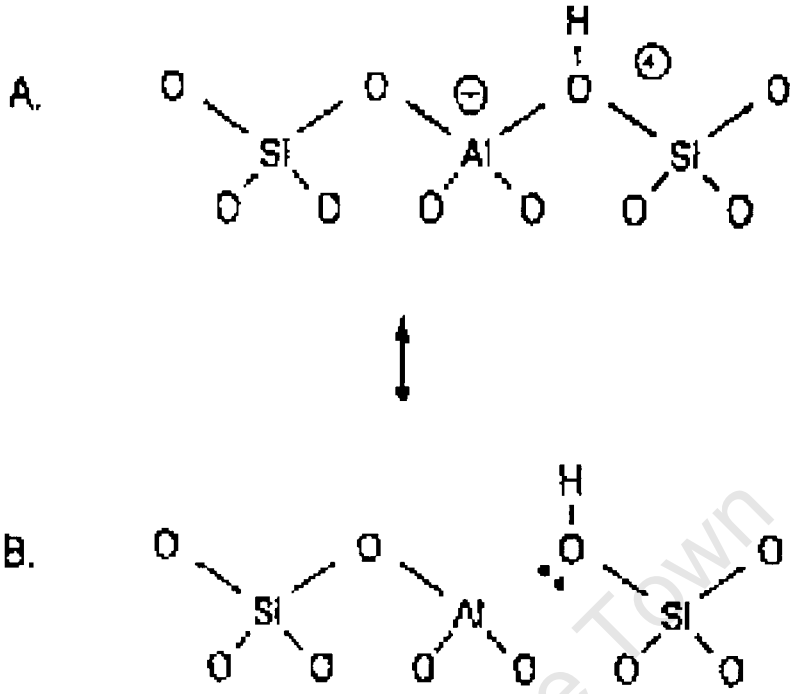

Figure 2.10: Visualization of a protonic (Brønsted) acid in a zeolite. (Venuto, 1994).

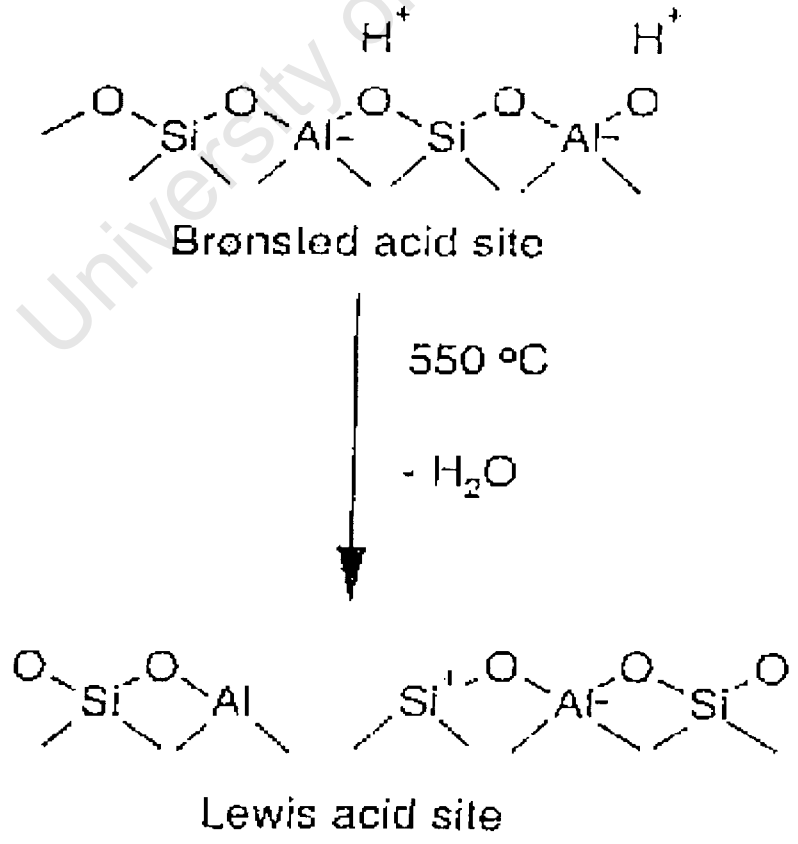

Figure 2.11: Formation of Lewis acid sites in zeolites (Stöcker 2005).

2.5.2 Zeolite catalysis

The proposed general acid-catalysis mechanism for the oligomerization of propylene over a solid acid catalyst is shown in Scheme 2.4 (O'Connor, 1997).

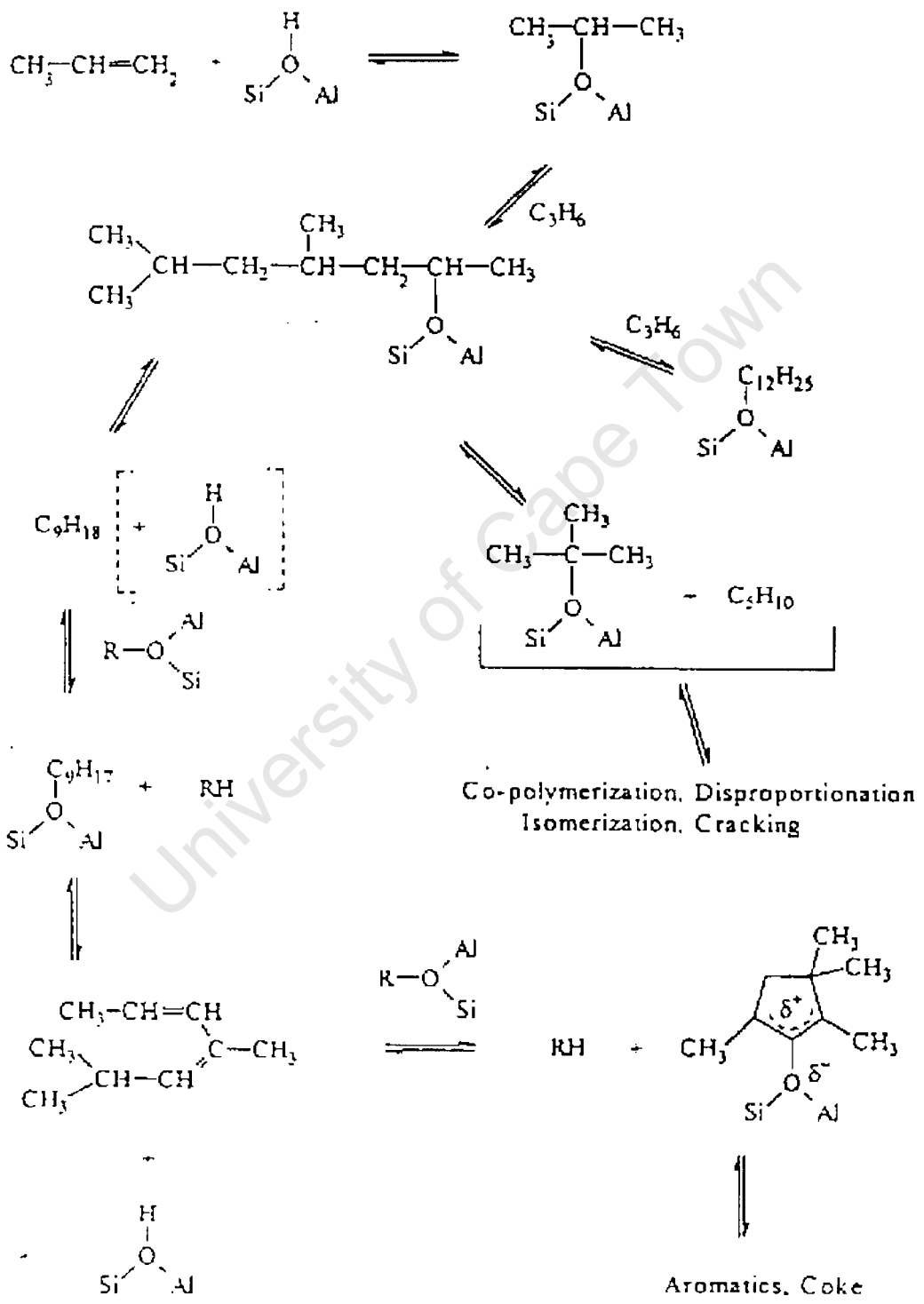

Scheme 2.4: Mechanism for propylene oligomerization over an acid catalyst (O'Connor, 1997)

The first step involves protonation of the olefin monomer by the Brønsted acid site. Subsequent monomer addition results in chain growth via a carbenium ion. Termination of the chain growth can occur as a result of proton transfer, thus regenerating the acid site in the catalyst. The olefin thus formed may undergo hydride transfer which ultimately results in the formation of dienes and aromatics. Alternatively copolymerization, disproportionation, isomerization and cracking can occur.

2.5.3 Zeolite coking/deactivation

Catalyst deactivation is a time-dependent decay of catalyst activity and/or selectivity that can ultimately be caused by a change in the number, nature, or accessibility of the catalyst sites. Coke is the term that is generally used to describe a variety of higher molecular weight materials formed within zeolite pores or on the external surface (Venuto, 1994). The types of organic material that may be referred as coke range from simple olefin oligomers or other species with low diffusivities that are either physisorbed or chemisorbed at acid sites, to highly aromatic, hydrogen deficient carbonaceous material that may be the end result of hydrogen-transfer processes and high-temperature reactions.

Small pore zeolites such as LTA exhibit a low coke-forming tendency since their narrow-pore channel systems inhibit formation of cycloparaffins and aromatics (Venuto, 1994).

In a study of coke formation over the medium-pore MFI zeolite during the oligomerization of ethylene, Dypurk et al. (Venuto, 1994) observed that the coke formed at higher temperatures, i.e. 375 – 447°C was largely aromatic, whereas, at low temperature (300°C) the coke consisted largely of oligomeric products. Karge et al. (Venuto, 1994) conducted a spectroscopic study on the formation of coke during ethylene polymerization over MFI zeolite. At temperatures below 127°C, there was evidence for alkenyl and polyenic carbocations. At higher temperatures, the presence of di- and poly-phenyl cations, polyalkyl aromatics, and polycyclic aromatics were detected. In contrast, large pore zeolites such as MOR do not have shape-selective constraints on the formation of aromatic coke precursors and rapid

deactivation of MOR during benzene ethylation, even at temperatures as low as 100°C has been reported. The rapid deactivation was attributed to olefin polymerization reactions, leading to coke formation. The difference in coke types that form on different zeolite types emphasizes the crucial impact of zeolite pore size and geometry on the reaction paths leading to residue or coke formation.

2.5.4 Zeolite shape Selectivity

Different types of shape selectivity may influence the mediation of organic reactions over zeolites. Shape selectivity by mass transfer discrimination arises when significant differences exist in the diffusivities of various reagent molecules with respect to the pore size/configuration for a given zeolite. The extreme form of this type of shape selectivity, namely the complete exclusion of a class of molecules from intracrystalline volume of the molecular sieve, is illustrated in Figure 2.12. Here, because of its large and bulky shape, the highly branched C_{13} isoparaffin reactant is denied access to the pore channel system and internal active sites of the zeolite, and passes through the catalyst bed unchanged. The linear paraffin is not excluded from entry to the pores, and undergoes reaction on the internal active sites.

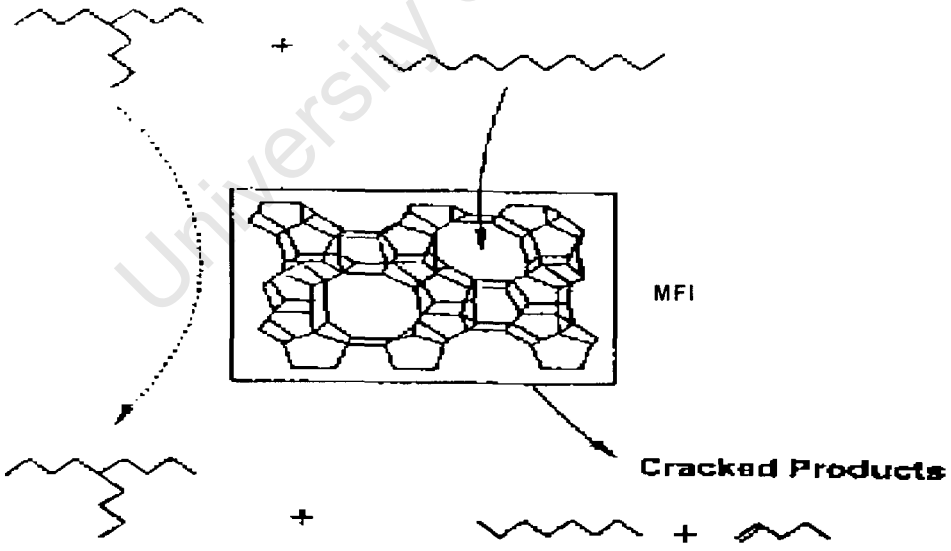

Figure 2.12: Schematic visualization of reactant selectivity for conversion of a mixture of linear and highly branched C_{13} paraffins over the medium-pore MFI (Venuto, 1994).

As shown in Figure 2.13, mass transport discrimination is not limited to total cutoff, but can effectively occur when several species can enter or leave the pores, but the diffusivity of one of the species is significantly higher than those of the others. In general, the above discrimination is referred to as reactant shape-selectivity.

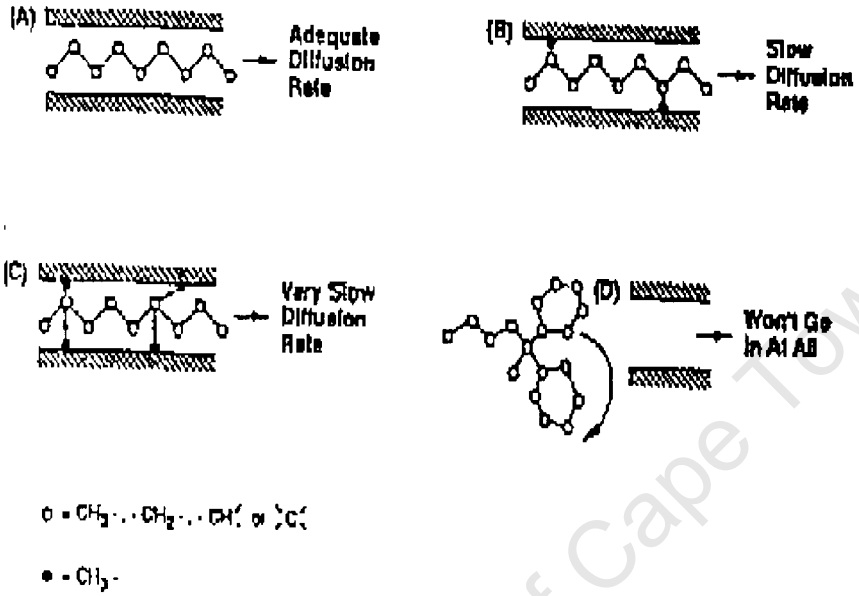

Figure 2.13: Simplified visualization of relationship between reactant structure and diffusivity for a medium-pore zeolite. The ultimate case is complete size exclusion (D) (Venuto, 1994).

Similarly, a shape selective effect can occur in relation to the reaction products, as shown in Figure 2.14, where certain isomers may preferentially leave the zeolite pore while others are retarded or, in extreme cases, trapped. Haag and Chen (1987) have reported excellent examples of the remarkable molecular discrimination attainable with the medium–pore MFI catalyst (Figure 2.15). Diffusivities for the hexanes drop sharply as one progresses from linear, to singly, to doubly branched isomers representing a span of > 10^3 in diffusivity. Likewise, o-xylene diffuses more than three orders of magnitude more slowly than p-xylene and the more bulky, symmetrical 1,3,5-trimethylbenzene encounters even more resistance. These effects are referred as product shape selectivity.

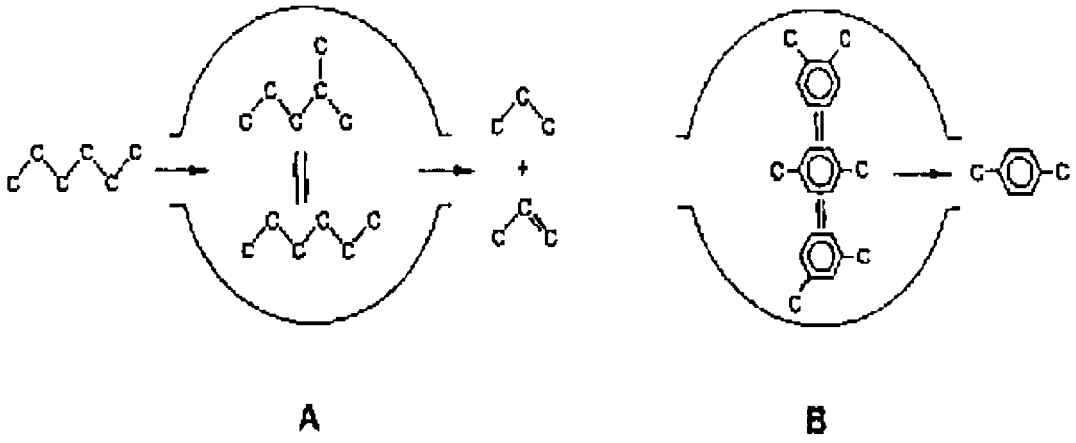

Figure 214: Schematic visualization of product exclusion for (A) small-pore zeolite and (B) medium-pore zeolite (Venuto, 1994).

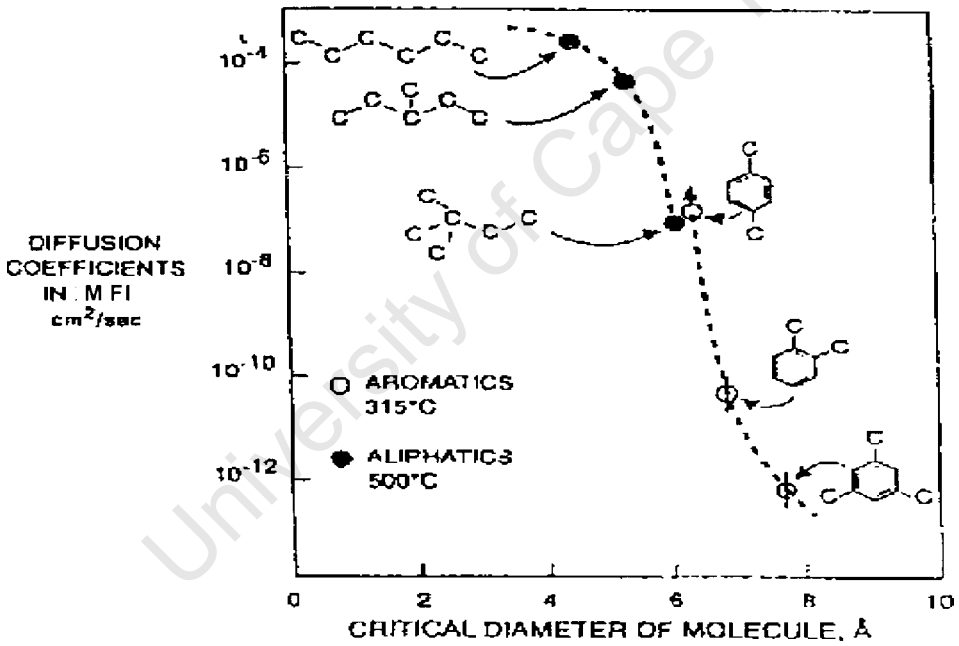

Figure 2.15: Duffusion coefficient in MFI for hexane isomers (at 500°C) and several aromatics (at 315°C) (Haag and Chen, 1987).

The third type of shape-selectivity is known as the restrictive transition-state selectivity (Figure 2.16). In this case, reaction pathways within zeolite microchannel systems can also be inhibited or blocked if the available space is insufficient to accommodate the steric or geometric demands of the required transition state or intermediates.

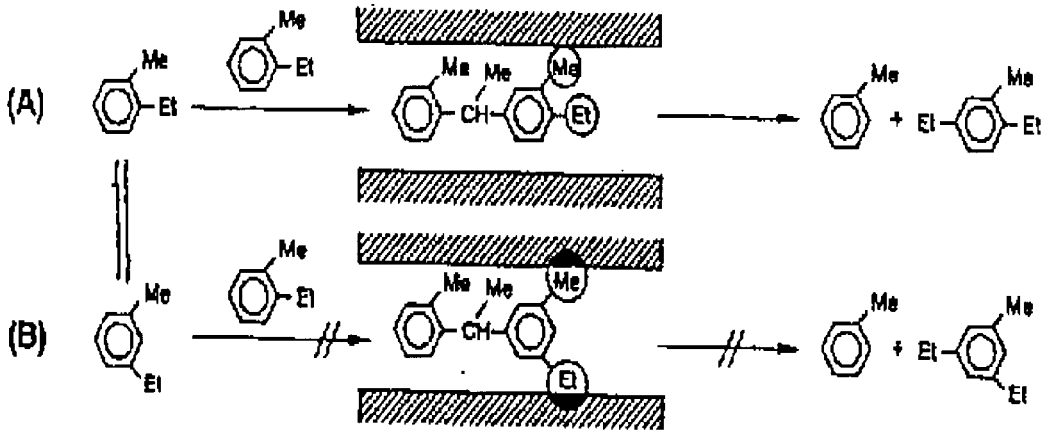

Figure 2.16: Conceptual example demonstrating restrictive transition –state in reaction of 1-methyl-2-ethylbenzene over MOR at 204 – 325°C. (A) Diarylalkane intermediate can be formed. (B) Geometric and volume requirement of diarylalkane intermediate are incompatible with available zeolitic pore space (Venuto, 1994).

2.5.5 External and internal sites versus shape selectivity of zeolites

Complete exclusion of a molecule from entering a zeolitic pore represents the extreme case of reactant selectivity. When reaction is found to occur in such catalytic systems, it may be assumed that the reaction occurred on the external surface of the zeolite (Venuto, 1994). Likewise, if huge, bulky, rigid product molecules are found, the dimensions of which clearly exceed the entry pore size of the zeolite in question, an assumption of external surface reaction is reasonable too. There is also reason to argue that external surface sites should show different strengths, concentrations and selectivities compared to fully tetrahedrally coordinated sites within the crystal interior (Venuto, 1994).

2.5.6 Surface deactivation (methods and findings)

The external (unrestricted) active sites of zeolites may have a noticeable impact on product distribution and the intrinsic selectivity. Therefore, various surface modification methods have been applied to enhance the selectivity of zeolites in hydrocarbon processing (Bauer et al., 2005, Blain et al., 1991, Chen et al., 2002, Ding et al., 2002, Giacobbe et al., 1992, 1993, Halgeri and Das, 2002, Hu et al., 1999, Kim et al., 1999, Klemm et al., 1998, Page et al., 1989, Purenago et al., 1993, Roger et al., 1997, Shaikh et al., 1999, Weber et al., 2000). Chemical vapour/liquid deposition of organosilicon compounds, pre-coking procedures and co-feeding with

bulky bases are reported to be the most effective ways to deactivate non-shape selective acid sites present on the external surface of zeolite crystallites.

In the silanization process, bulky alkoxysilanes such as tetraethoxysilane (TEOS), with a molecular diameter of about 0.96 nm, interact with external surface OH groups accompanied by the formation of the corresponding alcohol and the deposition of silica (after calcination) on the external surface. However, traces of water can hydrolyze TEOS, i.e. the shielding effect of the bulky ethoxy group is diminished by the formation of $Si(OH)_4$ which has a smaller kinetic diameter (ca. 0.5 nm). As a consequence, silica deposition in the pore-mouth region and within the zeolite channels may occur and which may in turn result in pore narrowing or blocking (Bauer and Freyer, 2005).

For modification by pre-coking, the zeolite catalyst is typically contacted with feedstock under high severity conditions during initial time-on-stream (Bauer and Freyer, 2005). However, uncontrolled coke deposition has the drawback of affecting active sites within the zeolite channels and reducing, thereby, the catalyst activity. For coke deposition on the external surface, a post-treatment of conventionally pre-coked samples by hydrogen is recommended (Bauer and Freyer, 2005). Such a hydrogen treatment at elevated temperature initiates partial hydrocracking, rearrangement and/or migration of 'coke' deposits. As a consequence, intracrystalline alkylaromatic coke may be effectively removed, whereas bulkier polyaromatic coke remains on the external surface.

In the case of external site elimination via co-feeding bulky basic compounds, such compounds having an effective cross-section larger than the zeolite pore are pre-mixed with the feed material, or pre-contacted with the zeolite before the catalytic reaction (Blain et al., 1991, Giacobbe and Ksenic, 1992, 1993, Page et al., 1989), pore narrowing or blockage may result, as described for the silanization process.

2.5.7 Reported effects of selective elimination of external surface sites.

In general, the elimination/deactivation of external acid sites should substantially suppress undesired secondary reactions occurring on the external catalyst surface and/or decrease the diffusivity of undesired reactants or products into or out of the

zeolite pores, respectively. Thus, deactivation of surface acid sites and/or narrowing of the effective pore openings may be expected to improve the shape selectivity of MFI type zeolites (Bauer and Freyer, 2005).

In the case of toluene and ethylbenzene disproportionation (Chen et al., 2002), as well as xylene isomerization (Bauer and Freyer, 2005), any expected enhancement of para-selectivity by pore narrowing may be diminished by undesired secondary disproportionation or isomerization reactions of the target product p-product on the external acid sites. Effects of surface modification by liquid-phase deposition of hydrolyzed TEOS and a modified pre-coking procedure on selectivity have been studied during the xylene isomerization over nano-sized Pt/MFI (Bauer and Freyer, 2005). While single cycle silanization led to inefficient deactivation of strong surface acid sites, the combination of pre-coking and post-treatment with hydrogen was found to facilitate elimination of external acid sites which are responsible for undesired disproportionation reactions during xylene isomerization.

Blain et al. (1991), Page et al. (1989) and Giacobbe and Ksenic. (1992, 1993) reported improved selectivity to mono-methyl branched oligomers during the oligomerization of propylene and 1-butylene over a surface modified MTT type zeolite.

3 OBJECTIVES OF THIS STUDY

It has been reported in the literature that shape-selective catalysts such as MFI (Kojima and O'Connor, 1990) and surface-deactivated TON (Blain et al., 1991, Giacobbe and Ksenic, 1992, 1993, Page et al., 1991,) are capable of limiting the degree of branching in the oligomers formed from C_3 – C_6 olefins. It is further claimed, that the degree of branching can be limited to one methyl branch for every 5 to 9 carbon atoms in the oligomer molecule and, in addition, that, due to the acid-catalysis mechanism the branching is directed towards the centre of the hydrocarbon chain.

This study, therefore, aims to evaluate the performance of commercially available medium pore zeolites (MFI and TON) in comparison to large pore (BEA) and non-shape-selective (amorphous silica-alumina) materials for the selective dimerization of 1-hexene to mid-branched olefin intermediates suitable for detergent alcohols with good biodegradability and cold water detergency. Based on the literature cited, catalytic performance is to be evaluated at conditions most suitable for dimerization without excessive side reactions, viz. low temperature (ca. 160 °C) and high pressure (ca. 30 bar).

Specifically, the study seeks answers to the following key questions:

1) Are commercially available medium pore zeolites suitable for the desirable dimer properties?
2) What is the influence of zeolite pore size and geometry on the extent of dimer branching?
3) What is the optimum zeolite silica/alumina ratio?
4) What are the optimum reaction conditions (temperature, pressure and WHSV)?
5) Does external surface deactivation substantially improve dimer properties, i.e. limit extent of branching?

4 EXPERIMENTAL

4.1 Catalysts and feedstock

98.9 % pure 1-hexene (Sasol) was used as feed for the olefin oligomerisation studies. Impurities comprised essentially double-bond and skeletal C_6 isomers.

Catalysts, listed in Table 4.1, were selected on the basis of SiO_2/Al_2O_3 ratio, pore size and structure, and a 'reference' solid acid catalyst without shape-selective properties (amorphous silica-alumina). It should be noted that whereas the catalysts employed are considered appropriate materials for the intended investigation, these materials are not necessarily designed or optimized by the manufacturers for the express purposes of hexene dimerization.

Table 4.1: Catalysts tested

Catalyst Sample	Common name	SiO_2/Al_2O_3 Ratio	Source
MFI-90	MFI	90	Süd-Chemie AG
MFI-120	MFI	120	Süd-Chemie AG
MFI-220	MFI	220	Süd-Chemie AG
MFI-400	MFI	400	Süd-Chemie AG
TON-90*	ZSM-22	90	Sasol
BEA-150	Zeolite β	150	Süd-Chemie AG
SA	Siral-40	1.13	CONDEA
MFI-90^e	MFI^e	90	Süd-Chemie AG

*Synthesised by Sakuneka (2004), e = extrudate form (all other samples in the form of powders)

SA = amorphous silica-alumina

Experiments aimed at the selective deactivation of the external surface of the MFI-90^e catalyst, involved the co-feeding of the following catalyst poisons: 2,4,6–collidine, 2,6–di-t-butyl amine and 4–methyl quinoline. All these bases were used as supplied by Sigma-Aldrich without further purification.

2,4,6-collidine

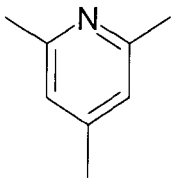

2,6-di-t-butyl amine

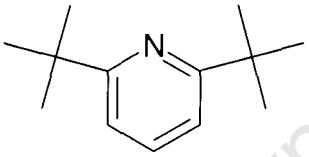

4-Methylquinoline

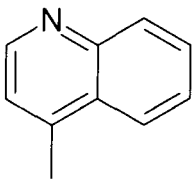

4.1.1 Feed purification

Feed purification was performed by passing approximately 2 litres of 1-hexene through a column packed with ca. 100 ml of activated neutral alumina (Sigma-Aldrich) to remove or minimise the amount of impurities (e.g. oxygenates) using the apparatus depicted in Figure 4.1.

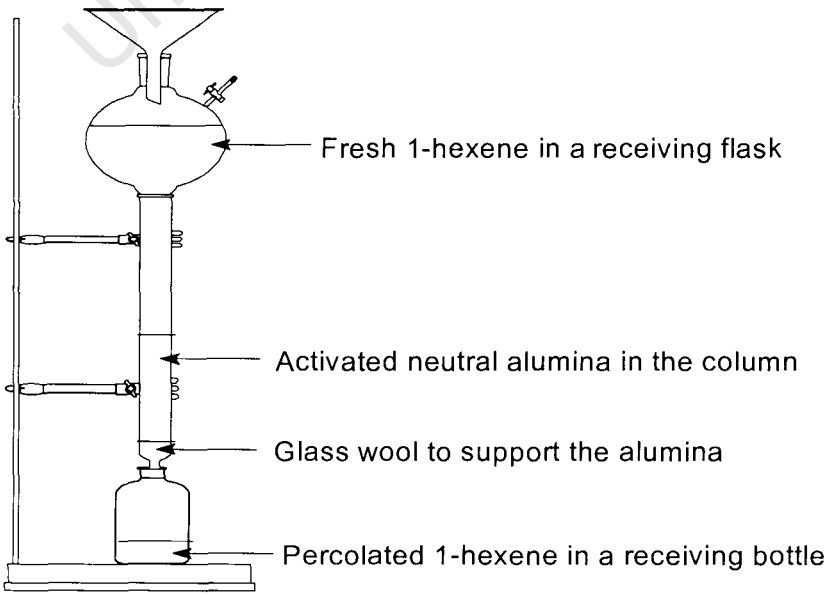

Figure 4.1: Set-up for the removal of feed impurities.

4.2 Catalyst test apparatus

4.2.1 Description of reactor system

Figure 4.2 represents a schematic flowsheet of the reactor system used for the dimerization of 1-hexene. The feed is supplied via an HPLC pump through the reactor in down-flow to the catch-pot were the gaseous and liquid products are separated. The major parts of the system are described below.

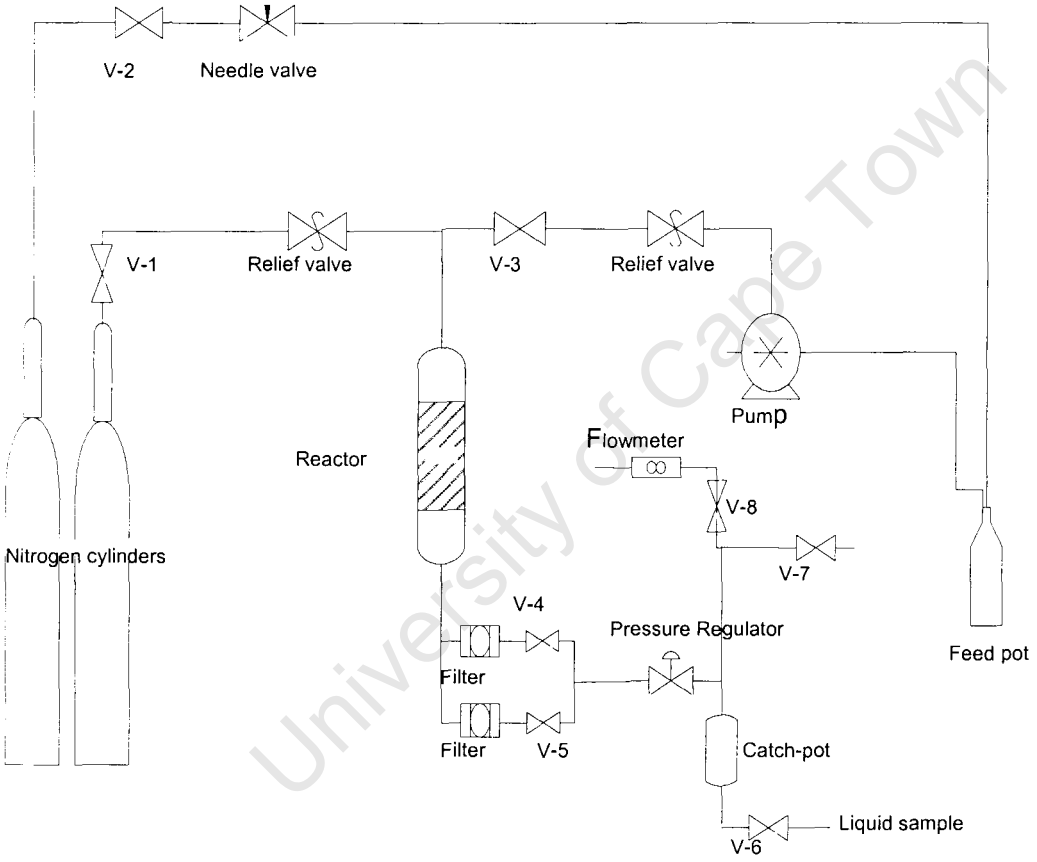

Figure 4.2: Reactor apparatus for 1-hexene dimerization.

4.2.2 Packed bed catalyst configuration and temperature profile

Under conditions of steady-state operation, the packed bed temperature profile was measured via an axial thermowell extending the full length of the reactor.

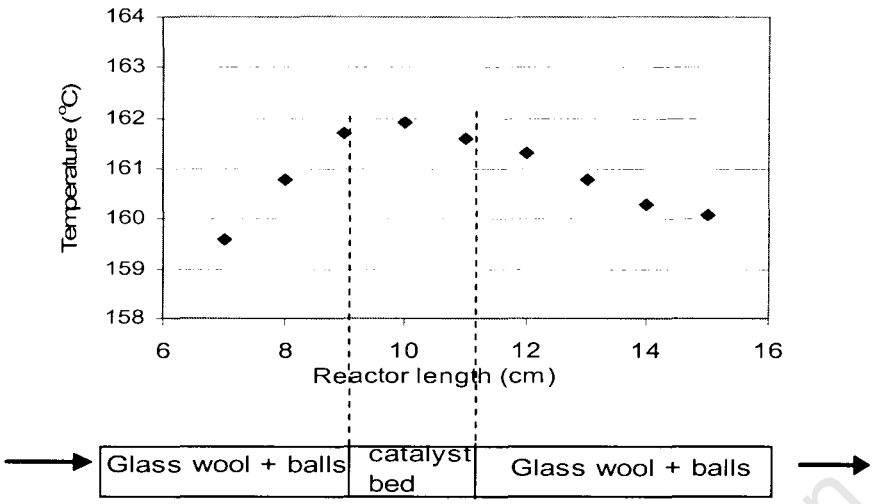

Figure 4.3: Temperature profile in the catalyst bed

As can be seen in Figure 4.3, the isothermal region within the reactor is approximate 1.5 cm long and extends slightly below and above the catalyst containing section.

4.3 Experimental operating procedures

4.3.1 Reactor loading

The desired mass of the catalyst was loaded into the middle of the reactor isothermal zone. Above and below the catalyst, 3 mm glass beads were used to fill up the dead volume and to facilitate plug flow behaviour. The typical configuration of the loaded reactor is as shown in Figure 4.4.

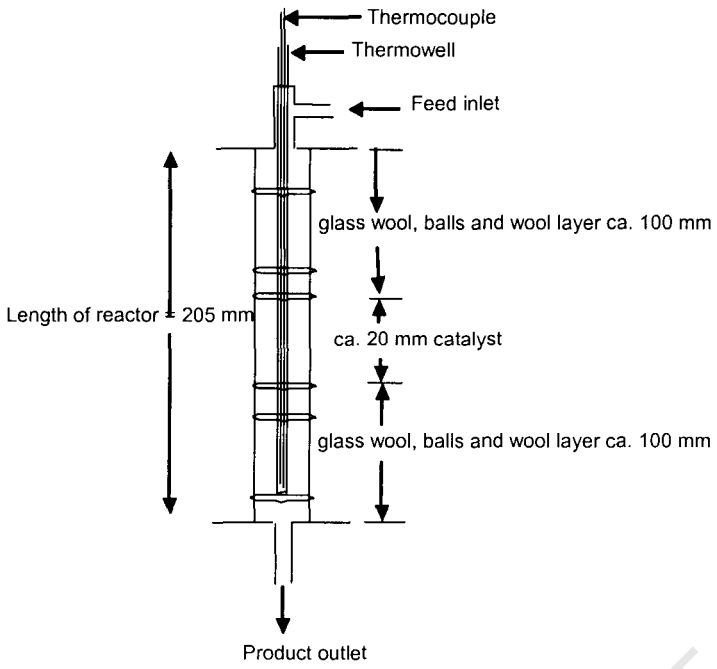

Figure 4.4: Loaded reactor configuration

4.3.2 Reactor leak test

Valves V-1 and V-3 (Figure 4.2) were opened to afford a flow of nitrogen into the reactor system. After catalyst loading and prior to activation, the reactor system was pressured to 10 bar above the intended reaction pressure. The absence of leaks was confirmed by soap bubble tests at all system connections and a static pressure test of at least 5 minutes.

4.3.3 Catalyst Activation

After completion of the leak test, the catalyst was activated under nitrogen flow (50 ml/min) at atmospheric pressure by raising the reactor temperature to 250°C for 1 hour, after which the temperature was reduced to the desired reaction temperature and the nitrogen flow discontinued. The catalyst remains isolated under nitrogen until the oligomerisation test is initiated.

4.3.4. Oligomerisation tests

4.3.4.1 Start-up procedure

The activated catalyst is brought on-stream by setting the back pressure regulator to the desired pressure followed immediately by pumping the feed at maximum pump speed (10 ml/min) to pressurise the reactor. Upon reaching the set pressure, the pump is set to the desired feed rate.

4.3.4.2 On-line procedures

The system was allowed to stabilise by monitoring system temperature and pressure. The expected volume from the pump was compared with the weight measured from the catch-pot contents for mass balance purposes.

4.3.4.3 Sampling

The catch-pot temperature was kept at about 0°C in order to limit the evaporation of any lighter materials which may have been present in the product. Liquid sampling was carried-out every 2 hours until stable conversion was observed, after which sampling was conducted twice daily.

4.3.4.4 Shut down procedures

At the end of each oligomerisation run, the pump was switched off followed by the setting of the back pressure regulator to atmospheric pressure. After depressurization, the system was purged with nitrogen for 5 hours at reaction temperature (to remove condensibles from the catalyst bed), after which the system was allowed to cool to ambient temperature under flowing nitrogen.

4.4. Standard operating conditions

The standard oligomerisation test conditions are provided in Table 4.2. The reason for operating under high pressure was to maintain liquid phase conditions.

Table 4.2: Standard reaction conditions

Activation:	
Temperature	250 °C
Flowrate of nitrogen	50 ml/min
Oligomerisation:	
Reaction temperature	160 °C
Reaction pressure	30 bar
Catalyst mass	2 g
1-Hexene WHSV	2.2 g/g.hr

4.5 Product work-up

4.5.1 Separation of the C_{12} fraction

The C_{12} (dimer) fraction was obtained from the bulk liquid product via distillation using the apparatus shown in Figure 4.5. The feed to the distillation column was put into RB1 and the system isolated from the atmosphere, followed by evacuation. The desired operating pressure was set by adjusting valve OV. Distillation was initiated by slowly increasing the reboiler temperature as required to achieve the desired fractions in RB2.

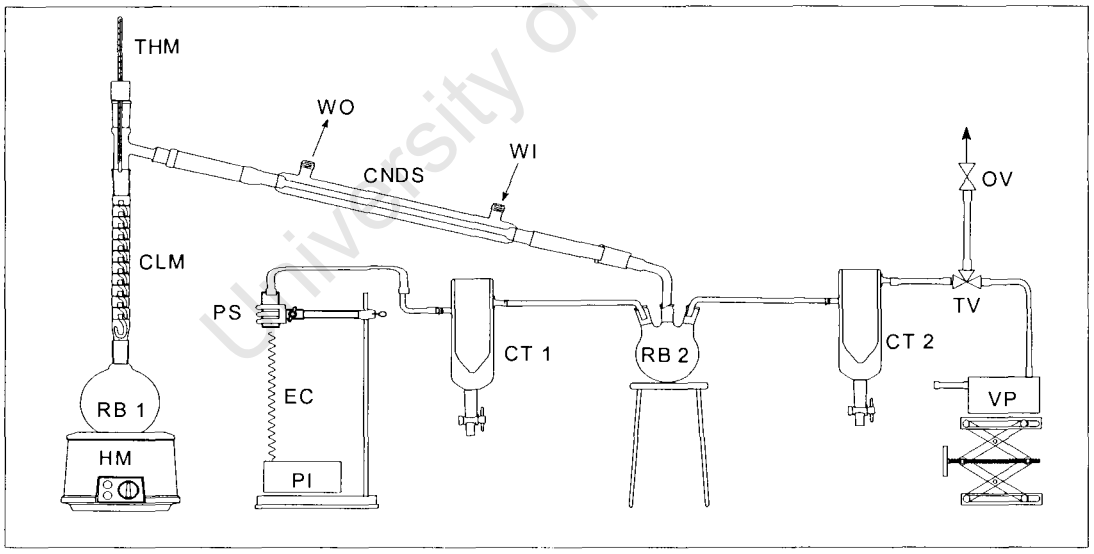

Key:

HM = Heating mantle **RB** = Round bottomed flask **CLM** = Column

THM = Thermometer **W** = Water **O/I** = out/in

CNDS = Condenser **PS** = Pressure sensor **EC** = Electrical conductor

PI = Pressure indicator **CT** = Cold trap **VP** = Vacuum pump

TV = Two-way valve **OV** = one-way valve

Figure 4.5: Micro-vacuum distillation set-up for hexene dimer separation.

4.5.2 Hydrogenation of the C_{12} fraction

The C_{12} fraction obtained from product separation was hydrogenated in order to simplify the resulting structural analysis by GC-FID, GC-MS and NMR using the apparatus shown in Figure 4.6. 5 – 10 g of dimer product was added to 300 ml of methanol and 10 wt % of a Pd/C catalyst (relative to dimer content) in a round bottomed flask fitted with a hydrogen reservoir (balloon). Hydrogenation proceeded overnight at room temperature under stirring (magnetic stirrer bar). The hydrogenated product was separated from the catalyst by passing the material through a column packed with neutral alumina, after which the methanol solvent was removed from the hydrogenated C_{12} fraction by rotary evaporation.

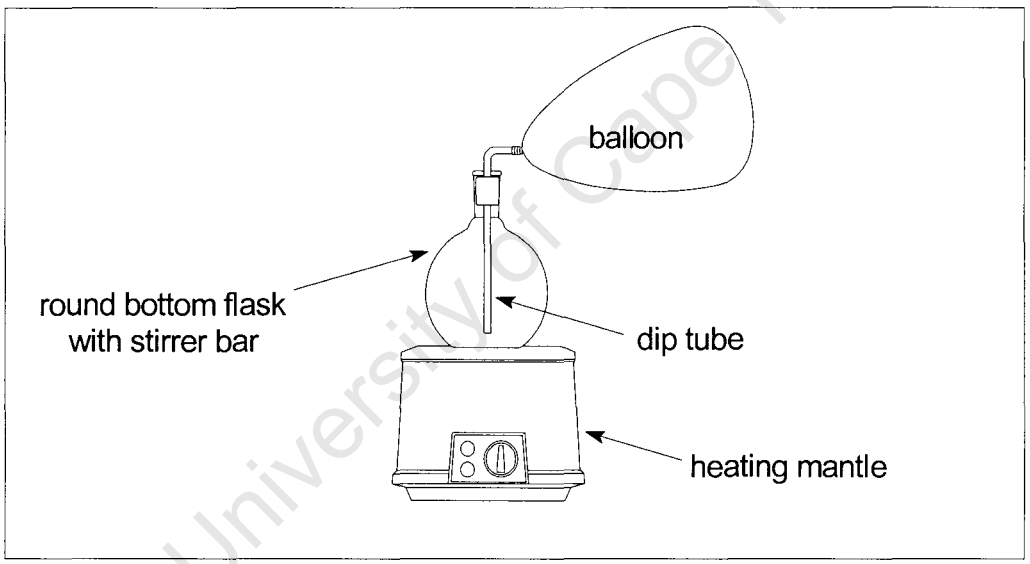

Figure 4.6: C_{12} hydrogenation apparatus

4.6 Product analysis and data work-up

4.6.1 Gas Chromatography (GC)

An HP 6890 series GC with flame ionization detector (FID) and a 50 m PONA (cross-linked methyl siloxane) column of 200 μm internal diameter and 0.50 μm film thickness was used for the analysis of the feed (1-hexene) and 1-hexene oligomerisation products. Full chromatographic conditions provided in Table 4.3.

Table 4.3: Chromatographic conditions for feed and product analysis

Operational parameter	Condition
Carrier gas	Nitrogen
Detector	FID
Column head pressure	140.3 kPa
Split ratio	100:1
Injector temperature	250 °C
Detector temperature	270 °C
Column temperature	70°C (5 min); 70 – 230 °C @ 8 °C/min; 230°C (25 min).

Figure 4.7 provides sample chromatograms of typical reaction products as well as reference standards.

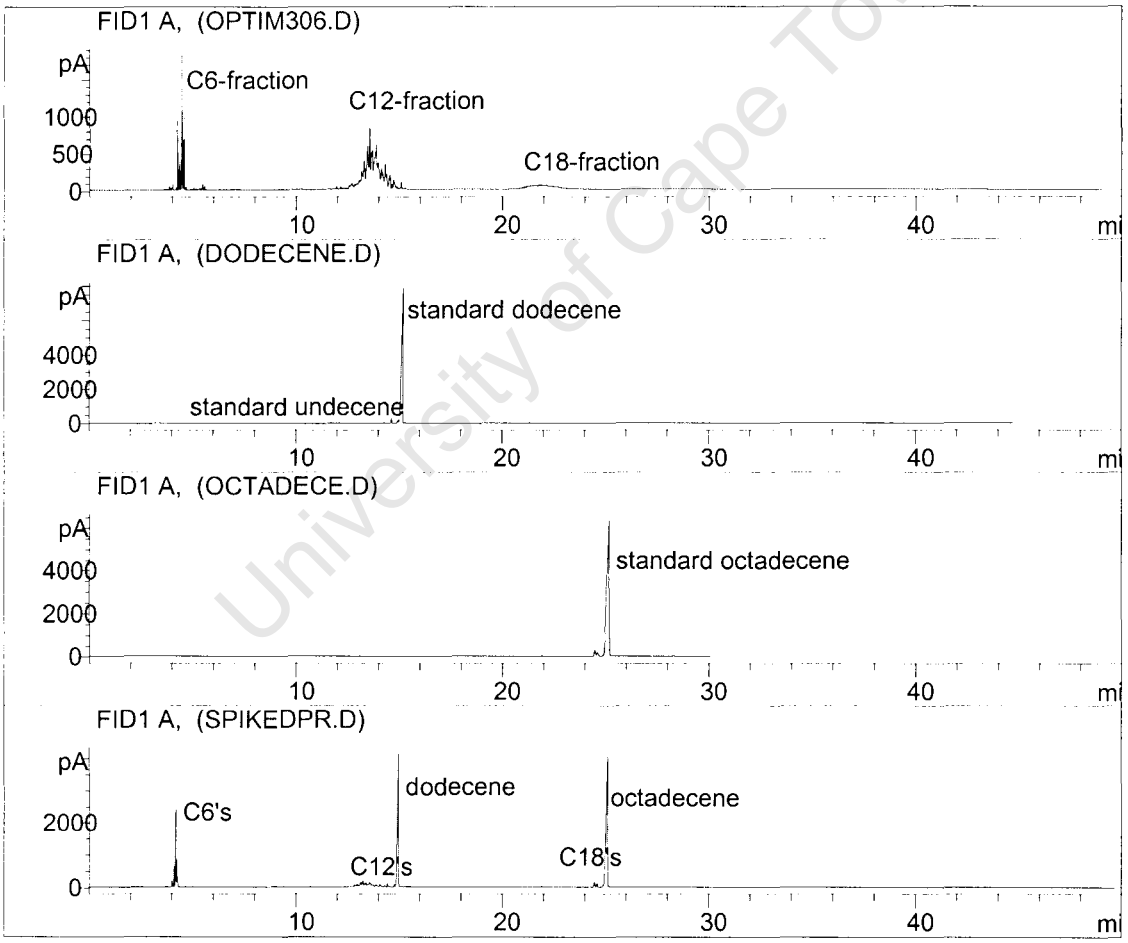

Figure 4.7: Chromatograms for the identification of the 1-hexene dimerization reaction products. [The chromatograms in order of appearance are; the typical reaction product, 1-dodecene contaminated with 1-undecene, pure octadecene and spiked reaction product]

Other sample chromatograms for the olefinic and hydrogenated C_{12} fractions are provided in Figures 4.8 and 4.9, respectively.

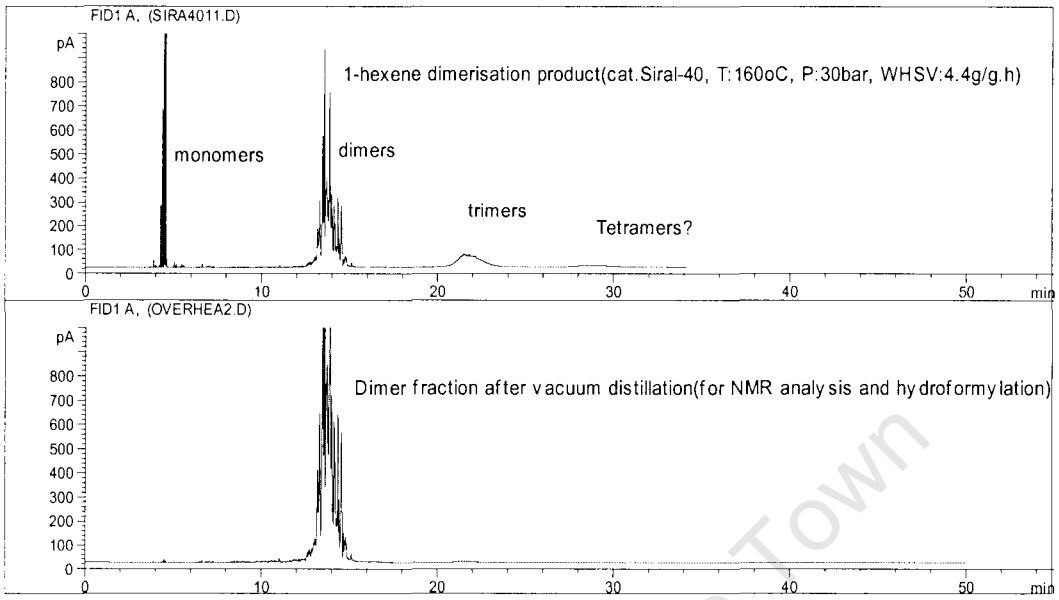

Figure 4.8: Sample chromatograms of the 1-hexene dimerization product and the distilled C_{12} fraction

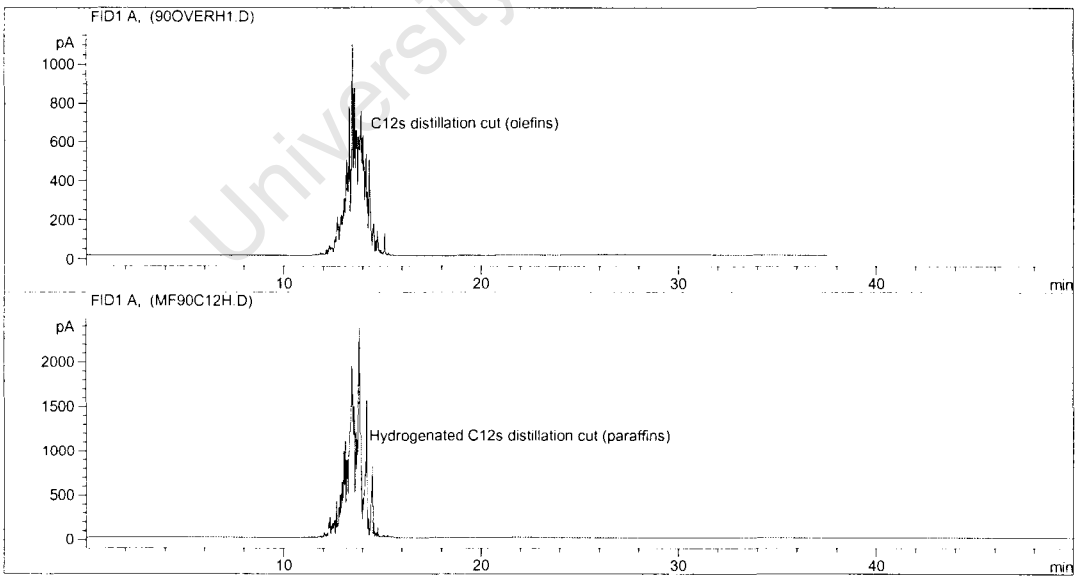

Figure 4.9: Sample chromatograms of the olefinic and paraffinic C_{12} fractions

Since both the feed and the product are olefinic, the FID relative response factors for all components are considered to be unity. Percentage conversion (X) of 1-hexene feed is calculated according to

$$X = \frac{F_{hexene,\,feed} - F_{hexene,\,product}}{F_{hexene,\,feed}} \times 100$$

and with all, FID response factors equal to unity, this reduces to

$$X = A_{hexene,\,feed} - A_{hexene,\,product}$$

since the feed is pure hexane and where F - flowrate and A – chromatogram area %.

Percentage dimer selectivity (S) and yield (Y) are calculated accordingly;

$$S = \frac{F_{dimers,\,product}}{F_{oligomers,\,product}}$$

$$= \frac{A_{dimers,\,product}}{A_{oligomers,\,product}} \times 100$$

$$Y \equiv \frac{X \times S}{100}$$

Note 1, in the above definitions, isomerisation of feed (1-hexene) is not considered to constitute conversion and, indeed, given that no measurable extent of cracking is observed (see Figure 4.8), conversion is effectively limited to oligomerisation.

Note 2, the above definitions provide selectivity and yield on a carbon % basis and not a mol % basis.

4.6.2 GC-MS

The same GC and column as described in section 4.6.1 were used except that in this case a 5973 network type mass selective detector (MSD) was employed instead of the FID. The main objective of this analysis was to identify the linear,

mono- and multi-branched fractions within the hydrogenated dimer product. The operating conditions of the GC were as outlined in Table 4.4.

Table 4.4: Operating conditions of the GC-MS

Operational parameter	Condition
Carrier gas	He
Detector	MSD
Column head pressure	152.3 kPa
Split ratio	200:1
Injector temperature	250 °C
Detector temperature	280 °C
Column temperature	70°C (5 min); 70 – 230 °C @ 8 °C/min; 230°C (25 min).

The identification of linear, mono- and multi-branched components in the hydrogenated dimers fraction was undertaken by comparing MS library suggestions with reported chromatographic analyses under identical conditions (Feulmer, 1986).

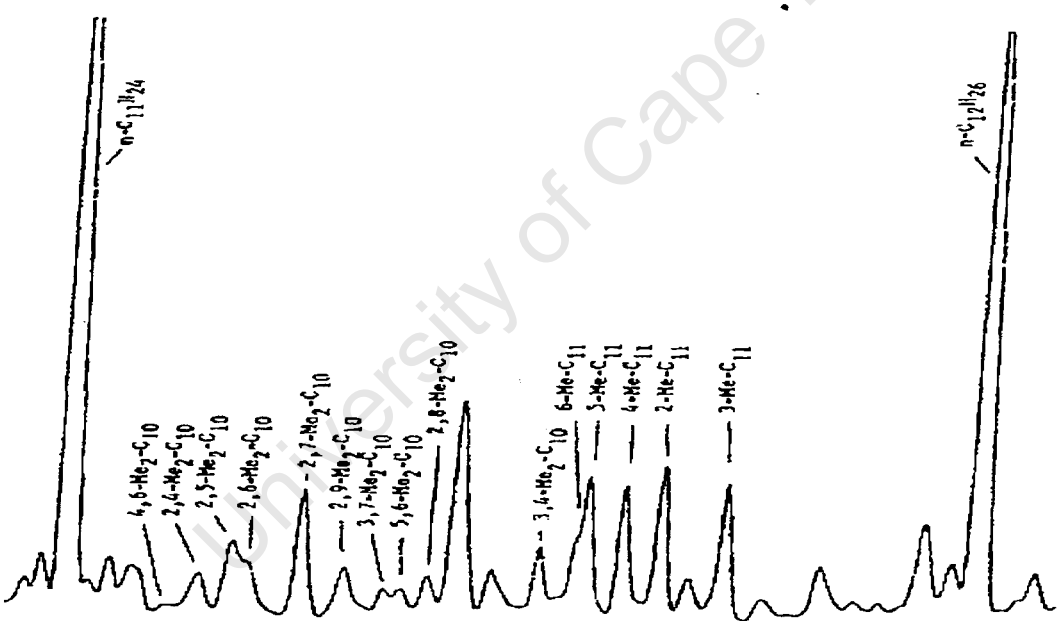

Figure 4.10: Gas chromatogram of a petroleum crude in the C_{11} – C_{12} range and the peak assignment for mono- and di-methyl substituted C_{12} alkanes (Feulmer, 1986).

The sample typical chromatogram of products of this study is provided in Figure 4.11.

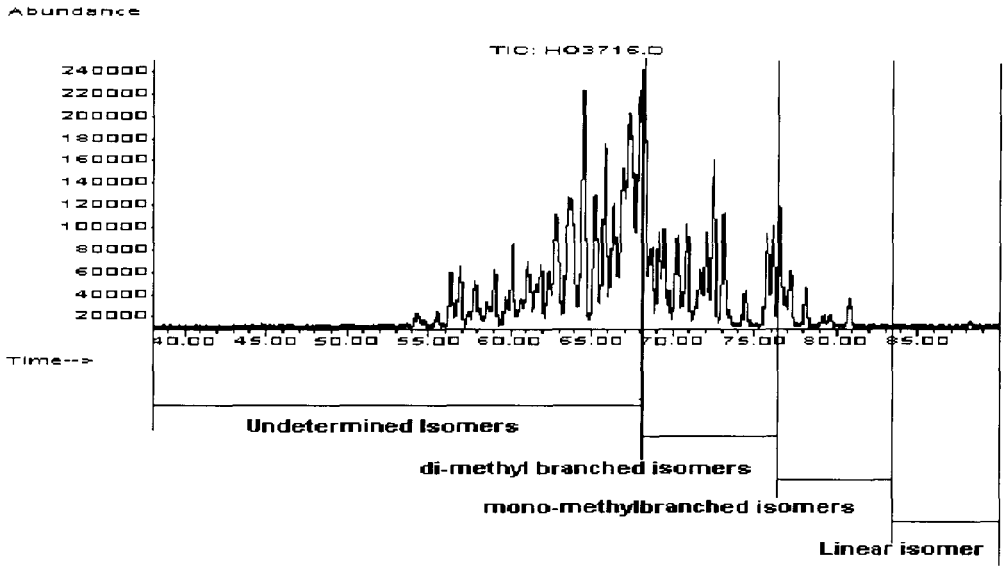

Figure 4.11: Chromatogram of hydrogenated C_{12} isomers

4.6.3 Analysis of hydrogenated C_{12} product by NMR

The hydrogenated C_{12} sample was dissolved in the minimum $CDCl_3$ (3ml sample and 0.5 ml $CDCl_3$) required to obtain a reference signal lock on the spectrometer. ^{13}C GASPE (Gated Spin echo) spectra were recorded with a 15 second relaxation delay. The method allows for identification of C, CH, CH_2 and CH_3 groups in the product C-skeleton via their distinctive J modulation resonance echoes (appendix C).

5 RESULTS AND DISCUSSION

A summarised listing of the experiments is provided in Table 5.1. In this Table, the catalysts were in two different forms as indicated by the superscript (e – extrudates and p – powder).

Table 5.1: Summary of experimental runs

Exp. #	Catalyst	Temperature (°C)	Pressure (bar)	WHSV* (g/g.hr)	Poison
1a	MFI-90^{p}	160	30	2.2	N/A
1b	MFI- 90 ^{p}	160	30	2.2	N/A
1c	MFI-90 ^{p}	160	30	2.2	N/A
2	MFI-90 ^{p}	160	30	4.4	N/A
3	MFI-90 ^{p}	160	30	6.6	N/A
4	MFI-120 ^{p}	160	30	2.2	N/A
5	MFI-220 ^{p}	160	30	2.2	N/A
6	MFI-400 ^{p}	160	30	2.2	N/A
7	MFI-90 ^{p}	160	30	4.4	N/A
8	BEA-150 ^{p}	160	30	2.2	N/A
9	TON-90 ^{p}	160	30	4.4	N/A
10	Siral-40 ^{p}	160	30	4.4	N/A
11	MFI-90 ^{e}	170	20	1.1	N/A
12	MFI-90 ^{e}	170	40	1.1	N/A
13	MFI-90 ^{e}	160	30	1.1	N/A
14	MFI-90 ^{e}	150	20	1.1	N/A
15	MFI-90 ^{e}	150	40	1.1	N/A
16	MFI-90 ^{e}	170	20	1.1	2,4,6-collidine
17	MFI-90 ^{e}	170	20	1.1	2,6-t-butyl pyridine
18	MFI-90 ^{e}	170	20	1.1	4-methyl quinoline

* WHSV based on zeolite content of the catalyst

5.1 Introductory experiments

The oligomerisation of 1-hexene was carried-out over MFI-90 as shown in Table 5.1, experiment 1a. The apparent initial increase in conversion indicated in Figure 5.1 during the first 35 hours on-stream is consistent with an artificial effect resulting from the system dead volume between the exit of the catalyst bed and the product catchpot, which is significant due to the test reaction being conducted in the liquid phase (or at the least with a substantial presence of liquid-phase components). A pseudo steady-state ensues accompanied by mild catalyst deactivation.

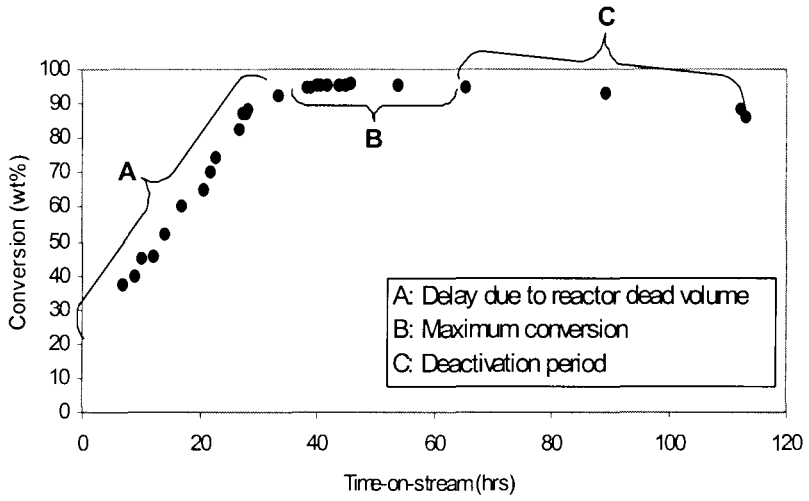

Figure 5.1: Conversion of 1-hexene versus time-on-stream for the dimerization reaction over MFI-90. [Experiment 1a]

A plot of dimer selectivity with time-on-stream is presented in Figure 5.2. Consistent with the observations for conversion, selectivity data prior to 35 hours-on-stream may be ascribed to artifacts associated with system dead volume. The subsequent increasing selectivity trend is consistent with a slowly decreasing conversion level with time-on-stream.

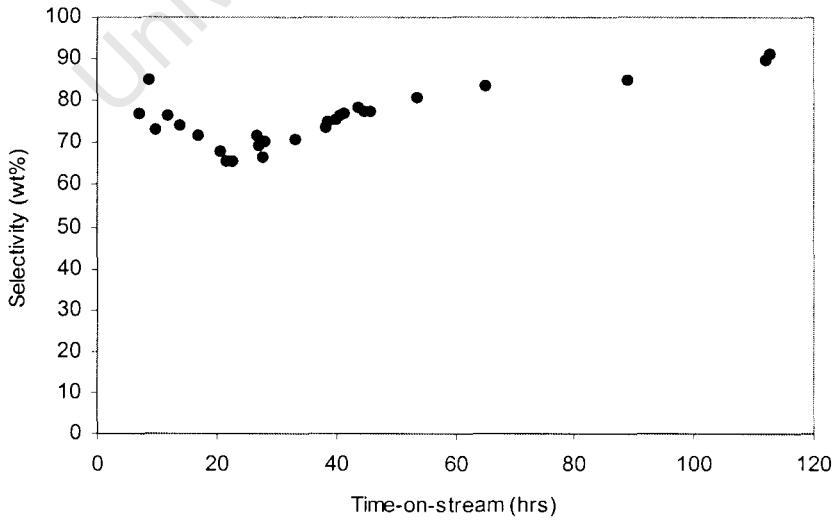

Figure 5.2: Dimer selectivity versus time-on-stream for the 1-hexene dimerization reaction over MFI-90 [Experiment 1a].

So as to avoid dead-volume affects, the interpretation concerning all further data presentation will exclude this early time-on-stream period.

5.2 Experimental reproducibility

Repeat experiments were conducted to evaluate experimental reproducibility. The results of 3 experiments are presented in Figures 5.3–4, from which it is apparent that the experimental reproducibility is acceptable.

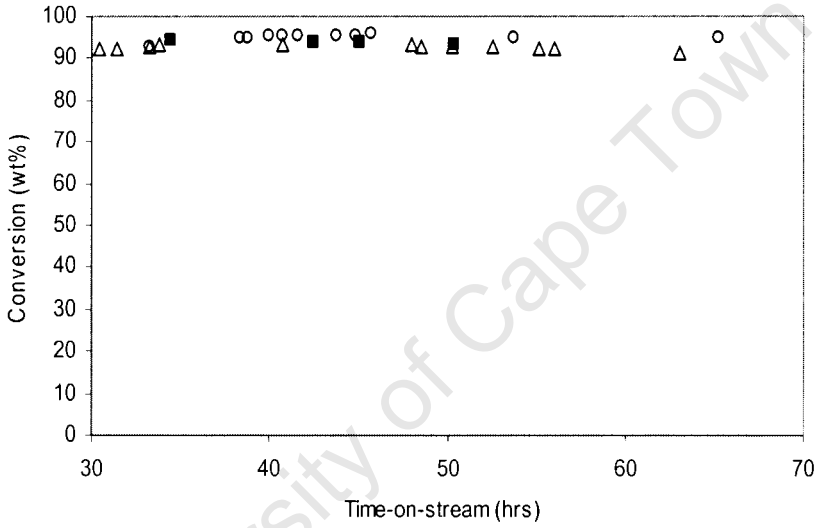

Figure 5.3: Reproducibility of conversion versus time-on-stream for the dimerization of 1-hexene over MFI-90. [Circles: Experiment 1a; Squares: Experiment 1b; Triangles: Experiment 1c]

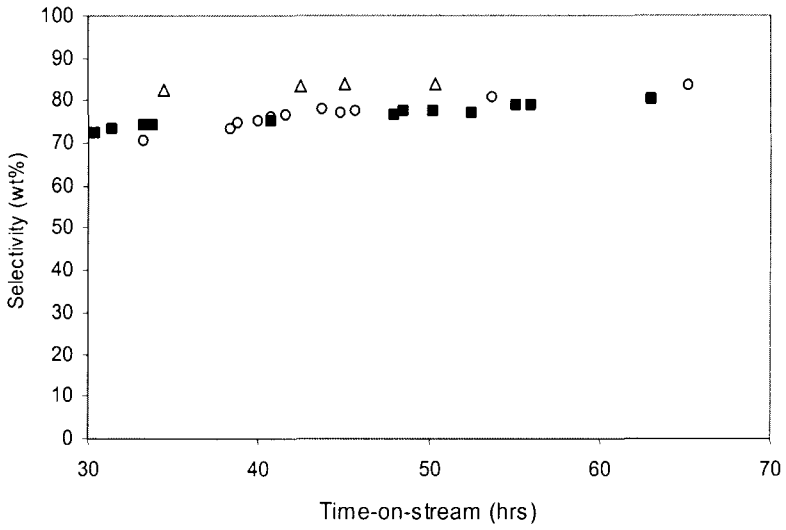

Figure 5.4: Reproducibility of selectivity to dimers versus time-on-stream for the dimerization of 1-hexene over MFI-90]. [Circles: Experiment 1a; Squares: Experiment 1b; Triangles: Experiment 1c]

5.3 Effect of contact time (WHSV) on conversion

The effect of contact time was investigated by varying the hexene feed rate, with a view to controlling the conversion range between 40 and 50 wt%. The results of these experiments are shown in Figure 5.5.

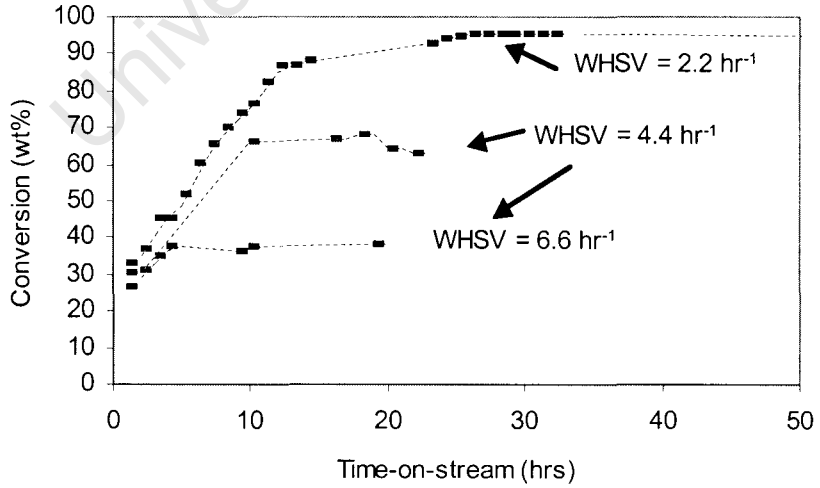

Figure 5.5: Conversion of 1-hexene versus time-on-stream at various WHSV's for the dimerization reaction over MFI-90. [Experiments 1; 2 and 3]

The conversion of 1-hexene decreases with a decrease in contact time as expected. It is also noteworthy that the lag time is shorter at the higher feed rates associated with increasing space velocity. A plot of dimer selectivity versus conversion (averaged at stable conditions) indicates that, under current test conditions of temperature and pressure, dimer selectivity is largely independent of conversion even to high conversion levels (~ 95 %) and , consequently, that high dimer yield may be achieved at these conditions (Figure 5.6).

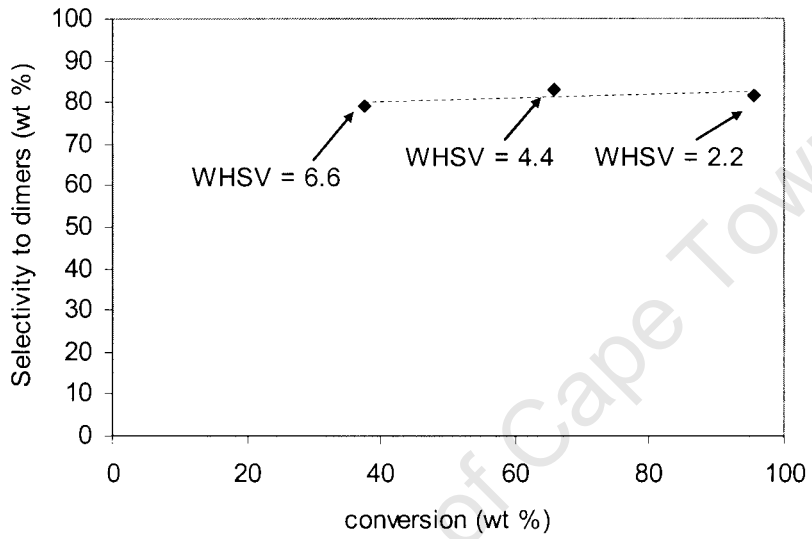

Figure 5.6: Average dimer selectivity versus average conversion of 1-hexene at various WHSV's for the dimerization reaction over MFI-90. [Experiments 1, 2 and 3]

5.4 Catalyst screening

In order to screen various catalyst types, both zeolite and amorphous silica-alumina, as well as different zeolite structure types, a set of experiments were conducted at standard conditions. However, depending on the activity of each catalyst, the contact time was adjusted accordingly in order to allow for catalyst comparison at similar conversion levels. The results of these experiments are presented in Figures 5.7–8.

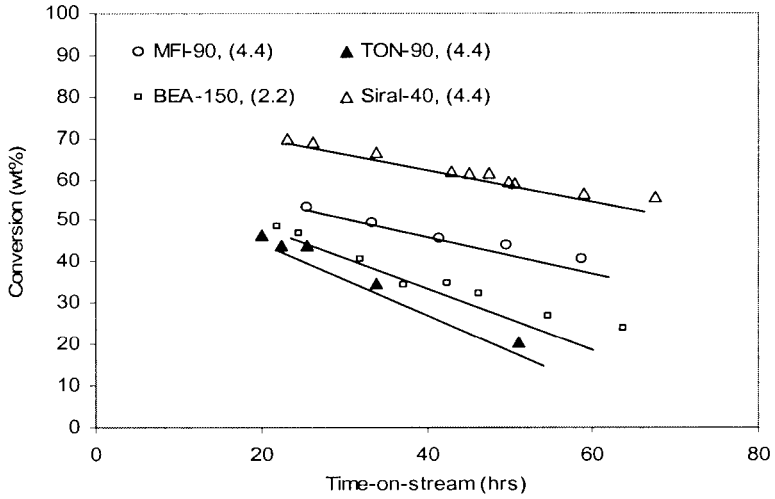

Figure 5.7: Conversion of 1-hexene versus time-on-stream for various catalysts at standard conditions but varying WHSV (g/g.hr) as indicated in parenthesis in the figure key. [Circles: Experiment 7; Open squares: Experiment 8; Solid triangles: Experiment 9; Open triangles: Experiment 10]

All catalysts show high initial activities with subsequent steady and similar deactivation behaviour. Taking the different test WHSV into account, it is possible to rank the catalysts in terms of declining activity as Siral-40 > MFI-90 > TON-90 > BEA-150, a result presumably influenced by a complex combination of each catalyst's relative acid-site density, strength and active site accessibility.

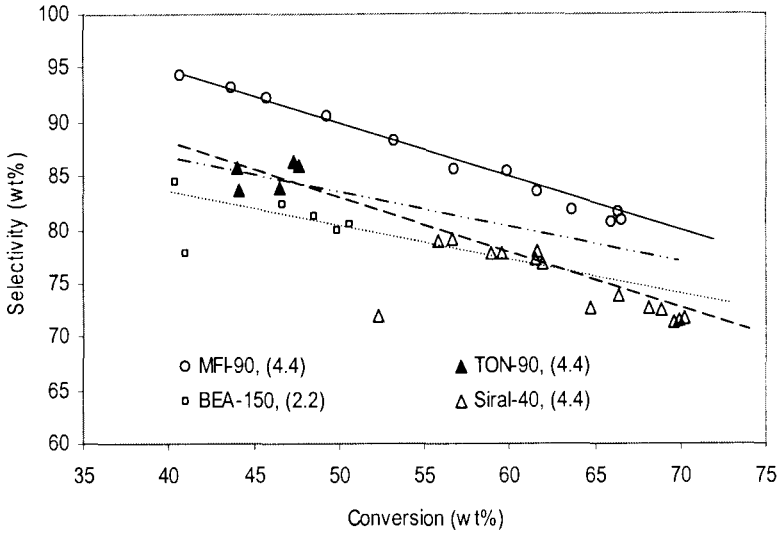

Figure 5.8 Dimers selectivity versus 1-hexene conversion for various catalysts (WHSV in parenthesis) [Circles: Experiment 7; Open squares: Experiment 8; Solid triangles: Experiment 9; Open triangle: Experiment 10]

Throughout the 40 – 70% conversion range dimer selectivity is consistently higher for MFI-90 as compared to the other catalysts of the test series (Figure 5.8). Collectively, from the above results it would appear that MFI-type zeolite is superior to the other catalyst types tested based on stability (section 5.1), dimer selectivity (Figure 5.8), activity (Figures 5.1 and 5.5) and commercial availability. It is, however, not clear from the results of Figure 5.8 whether other zeolite (TON-90 and BEA-150) are more selective than the amorphous catalyst (Siral-40). Nonetheless, amongst the zeolite catalysts, dimer selectivity appears to decline as MFI-90 > TON-90 > BEA-150.

NMR and GC-MS analyses of hydrogenated dimer product fractions are presented in Tables 5.2 and 5.3, respectively. It is apparent that all catalysts produce branched products, predominantly multi-branched (i.e. with two or more branches per C_{12} molecule).

GC-MS data suggest the average extent of branching to be roughly 2,6 – 2,7 branches/molecule for all zeolites and the amorphous silica-alumina catalysts. Similarly, the NMR data also shows a similar average branching extent, albeit lower at approximately 2 branches /molecule, except for TON which is substantially higher

at 3,2. The reason for the exceptional value in respect of TON is not clear but should be noted that these analyses were not repeated.

Table 5.2 NMR analyses of hydrogenated dimer products

	TON-90	BEA-150	SIRAL-40	MFI-90
No. of CH3's/molecule	5.24	4.02	4.17	4.04
No. of extra CH3s per molecule	3.24	2.02	2.17	2.04
No. of quaternaries/molecule	0.21	0.06	0.06	0.07

Table 5.3 GC-MS analyses of the hydrogenated C_{12} fractions

Catalyst	Multi-branched (wt%)	Di-methylbranched (wt%)	Mono-methylbranched (wt%)	Average branching
MFI-90	73	24	3	2.7
BEA-150	70	27	3	2.7
TON-90	73	16	9	2.6
Siral-40	64	31	5	2.6

Average number of branches per molecule calculated as(x%Mono + 2y%Di + 3z%Multi)/300 where multi-branched component is considered as tri-methyl branched.

5.5 Effect of SiO_2/Al_2O_3 ratio for the MFI-type catalysts

The influence of catalyst SiO_2/Al_2O_3 ratio on hexene dimerization performance is presented in Figure 5.9 for the preferred, MFI-type catalyst.

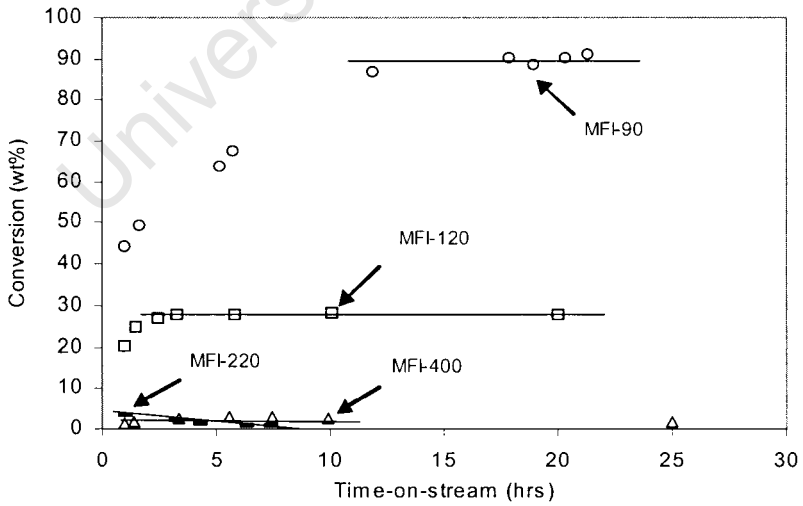

Figure 5.9: Conversion of 1-hexene versus time-on-stream for MFI type zeolites with different SiO_2/Al_2O_3 ratio. [Circles: Experiment 1; Squares: Experiment 4; Triangles: Experiment 5; Dashes: Experiment 6]

From figure 5.9, it is apparent that the activity of MFI catalyst for hexene dimerization is strongly influenced by zeolite SiO_2/Al_2O_3 ratio, lower ratios (greater active size density) resulting in higher activity. For the SiO_2/Al_2O_3 ratios tested activity declined as: MFI-90 > MFI-120 > MFI-220 ≈MFI-400 as may be expected on the basis of the number of sites available in each catalyst.

5.6 Effects of temperature and pressure on 1-hexene dimerization over MFI-90^e

Selecting MFI-90 as the preferred catalyst for hexene dimerization, the influence of temperature and pressure on overall dimerization performance was evaluated via a set of factorial experiments as indicated in Figure 5.10.

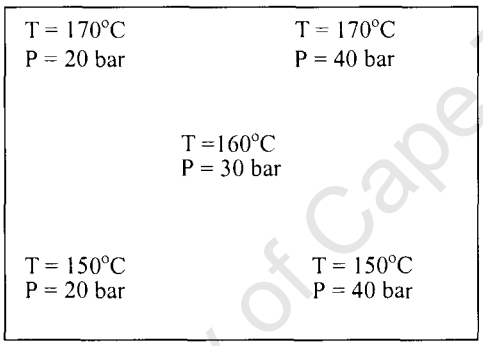

Figure 5.10: Reaction conditions for the 2-factorial design experiments

Additionally, these tests we performed on the industrial form of the catalyst, viz. in the form of 1/16" extrudates comprising 20 % alumina binder and 80 % zeolite, and consequently the catalyst is designated MFI-90^e. Space velocities indicated in the case of MFI-90^e catalysts are adjusted for binder content and reflect WHSV based on zeolite content only.

Hexene conversion versus time-on-stream and selectivity to dimer as a function of conversion are provided in Figures 5.11 – 12, respectively. From Figure 5.11, it can be seen that at the higher temperature of 170°C catalyst stability is substantially improved. In addition, conversion is largely insensitive to pressure at 170°C, whereas, at the lower temperature of 150°C the influence of pressure appears significant.

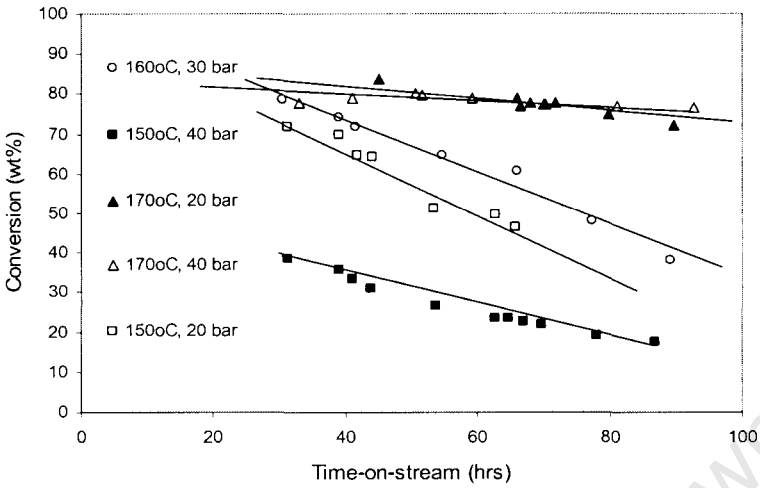

Figure 5.11: Hexene conversion versus time-on-stream over MFI-90^{e} catalyst. [Solid triangles: Experiment 11; Open triangles: Experiment 12; Circles: Experiment 13; Solid squares: Experiment 14; Open squares: Experiment 15].

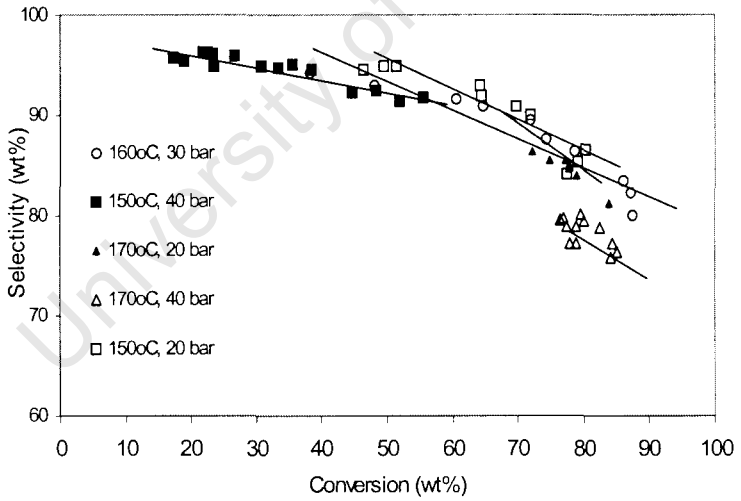

Figure 5.12: Dimer selectivity as a function of conversion over MFI-90^{e}. [Solid triangles: Experiment 11; Open triangles: Experiment 12; Circles: Experiment 13; Solid squares: Experiment 14; Open squares: Experiment 15]

In general, dimer selectivity declines with increasing conversion which is to be expected for a sequential (oligomerisation) reaction and, consequently any direct influence of

temperature on dimer selectivity is difficult to discern. However, from Figure 5.12, it would appear that higher pressure decreases dimer selectivity (data at 80 % conversion and 170°C) as may be expected. Even so, it is clear that selectivity is principally related to conversion and that temperature and pressure effects on dimer selectivity are largely secondary effects of conversion.

5.7 Effects of MFI-90^e external surface deactivation

In an attempt to further limit the extent of branching in the dimer product fraction, a selective deactivation of the external surface of MFI-90 crystallites was undertaken by the introduction of a poisoned feed (65 ppm N-poison in 1-hexene) to the operating catalyst. Results are presented in Figure 5.13, from which it is apparent that, upon base introduction deactivation is rapid and severe.

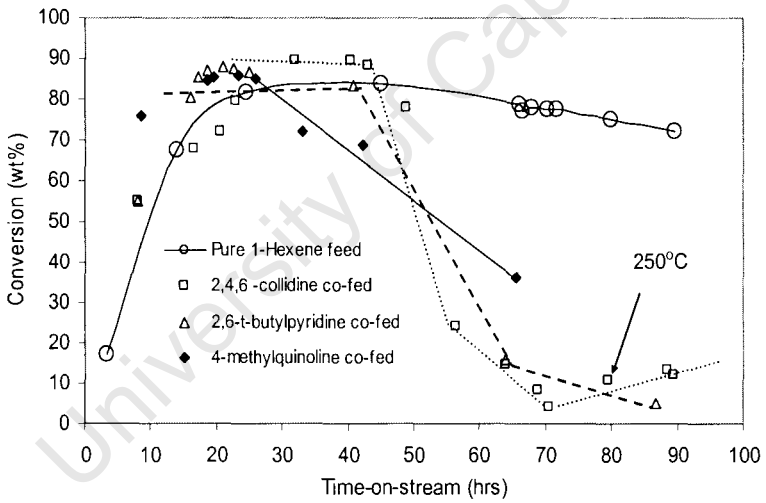

Figure 5.13: Conversion versus time-on-stream for poisoned and un-poisoned MFI-90^e catalyst at 170°C, 20 bar and 1.1 WHSV. [Circles: Experiment 11; Open squares: Experiment 16; Open triangles: Experiment 17; Solid squares: Experiment 18].

Catalyst activity appears to decline more rapidly, the accessible the nitrogen group on the basic compound i.e. 2,4,6-trimethylpyridine > 2,6-t-butylpyridine > 4-methylquinoline. An increase in temperature to 250°C (experiment 16) in the case of 2,4,6-collidine did not result in any significant recovery of activity. Chromatographic analyses of the product

samples taken in the presence or absence of poison show no indication of any shape selectivity to less branched dimer, when the nitrogen base is present.

6 SUMMARY AND CONCLUSIONS

For the purpose of producing mid-chain mono-methyl branched olefins, a range of acid catalysts were screened for the dimerization of 1-hexene, under generally mild conditions, viz. 150 – 170°C, 20 - 40 bar and 1 – 4h^{-1} WHSV. In general, catalysts exhibited a slow but steady decrease in conversion and a corresponding increase in dimer selectivity with increasing time-on-stream. Repeat experiments demonstrated an acceptable degree of experimental reproducibility.

Taking the different test WHSV's into account, it was possible to rank the catalysts in terms of declining activity as follows: amorphous silica-alumina > MFI-90 > TON-90 > BEA-150, presumably reflecting a complex combination of each catalyst's relative acid-site density, acid strength and active site accessibility. Dimer selectivity decreases with decreasing conversion above 40% as may be expected and generally dimer selectivity decreases as MFI-90 > Ton-90 ≈BEA-150 ≈amorphous silica-alumina.

NMR and GC-MS analyses of hydrogenated dimer product fractions indicated that all catalysts produce branched products, and that these products are predominantly multi-branched (i.e. with two or more branches per C_{12} molecule). With the possible exception of TON (NMR data only), the extent of dimer branching appears to be similar for all catalysts, although NMR data indicates a significantly lower degree of branching (2 branches/molecule) than does the GC-MS findings (2,7 branches/molecule). Given the degree of uncertainty implicit in the GC-MS branching fractions, it is suggested that the NMR branching ratio of two is more robust. The high TON branching observations from NMR is probably best considered erroneous in the absence of repeat experiments. Overall, therefore, the findings of this study suggest a similar degree of 2 for all catalysts. Moreover, given the mild conditions (low temperatures in the range 150 – 170°C) of this study, a branching ratio of two is consistent with an expected primary product from hexene dimerization without any prior or subsequent skeletal isomerization (Pater et al., 1999). The MFI-type zeolite appeared to be the catalyst of choice based on a combination of stability, activity and dimer selectivity. In addition, it is readily available on large scale. For

SiO_2/Al_2O_3 ratios tested activity declined as follows: MFI-90 > MFI-120 > MFI-220 ≈MFI-400, which may be expected on the basis of the number of Brønsted sites available in each catalyst.

The effect of temperature and pressure on stability, selectivity and activity of MFI-90 was further investigated. At higher temperatures (170°C) catalyst stability was substantially improved, and pressure did not appear to have a significant effect on conversion. However, at lower temperatures (150°C), increasing pressure led to significantly decreasing conversions.

Selective poisoning of the external surface of the MFI-90 catalyst using bulky bases effectively d the catalystic activity, suggesting that in the case of MFI zeolite, the hexene dimerization reaction occurs largely (if not exclusively) on the external crystal surfaces which are not shape-selective.

Concluding remarks

The sensitivity of the catalyst activity to pressure at 150°C is rather unusual and in the absence of repeat experiments, the findings of this study in terms of influence of pressure should be treated with circumspection. In general, pressure should not have such a significant effect on catalyst activity in this reaction medium (liquid phase).

The MFI-90 poisoning studies strongly suggest that in the case of this catalyst the catalytic activity of the catalyst may be completely passified by introduction of any of the three base molecules applied. As all these basic molecules have average kinetic diameter significantly larger than the MFI pore diameters of 5,1 X 5,5 Å and 5,3 X 5,6 Å, it is reasonable to deduce that the hexene dimerization reaction is catalyzed largely (if not exclusively) by the external surface sites of the MFI crystallites. In support of this argument, earlier studies by Corma et al. (1998) and by Lucas et al. (2001) have shown 2,6 –di-tert-butylpyridine and 2,4,6-collidine, respectively, not to enter the MFI pore system.

On the contrary, both Anderson et al. (1989) and Quann et al. (1988) claim hexene dimerization to occur within the MFI pores, although their experiments were conducted at significantly higher temperatures. On this basis, it may reasonably be argued that also in the case of the TON catalyst, with its nominal 4,6 X 5.7 Å pore diameter, the dimerization reaction must be attributed to external surface acid sites. In the case of BEA catalyst, it is likely that dimerization occurs within the pore system, but here the pore diameter maybe sufficiently large not to induce a shape selective constraint.

Certainly, for Siral-40 there are no shape selective constraints to be considered hence, the apparent insensitivity of dimer branching ratio with catalyst type observed may possibly be ascribed to the absence of shape selective constraints being operative. BEA and Siral pore being too large to induce shape selectivity and MFI and TON dimerization being limited to the external, non-selective, surface sites, the production of mono-methyl branched 1-hexene dimers could not be accomplished.

It is recommended that this work should be repeated in vapour phase medium in order to improve the diffusivity of 1-hexene and the dimer product in and out of the zeolite pore. This should enhance the expected shape-selectivity in zeolite catalyzed dimerization of 1-hexene.

REFERENCES

Anderson, JR, Chang, YF & Western, RJ 1989, 'Retained and desorbed products from reaction of 1-hexene over MFI zeolite: routes to coke precursors', *Journal of Catalysis*, vol. 118, pp. 466 - 482.

Battersby, NS, Kravetz, L & Salanitro, JP 2000,'Effect of branching on the biodegradability of alcohol-based surfactants', 5th *World Surfactants Congress, May 29 – June* 2, Florence. Proceedings, Vol. 2, pp. 1397-1407.

Bauer, F, Bilz, E & Freyer, A 2005,'C_{14} studies in xylene isomerization on modified HMFI', *Applied Catalysis A: General*, vol. 289, pp. 2 – 9.

Bekker, R & Kirk, M 2003, Internal Report (AT0431C, AT0432C, AT0466C, AT0467C, AT0647C), *'Analysis of four C_{12} cuts produced by dimerization of hexene using four different catalysts'*, Sasol Technology R&D.

Blain, DA, Page, NM & Young, LB (Mobil Corporation) 1991, *Olefin oligomerisation with surface modified zeolite catalyst*, US patent 5 026 933.

Calvin, JR, Davis, RD & McAteer, CH 2005,'Mechanistic investigation of catalysed vapor-phase formation of pyridine and quinoline bases using 13CH2O, CH3OH and deuterium-labeled aldehydes, Vol. 285, pp 1 – 23.

Chen, WH, Tsai, TC, Jong, SJ, Zhao, Q, Tsai, CT, Wang, I, Lee, HK & Liu, SB 2002,'Effects of surface modification on coking, deactivation and para-selectivity of HZSM-5 zeolites during ethylbenzene disproportionation', *Journal of Molecular Catalysis A*: Vol. 181, pp. 41 – 55.

Cookson, DJ & Smith, BE 1981. 'Improved methods for assignment of multiplicity in ^{13}C NMR spectroscopy with application to the analysis of mixtures', *Organic Magnetic Resonance*, Vol. 16, no. 2, pp. 111 - 116.

Corma, A, Fornes, V, Forni, L, Marquez, F, Martinez-Triguero, J & Moscotti, D 1998,'2,6-Di-Tert-Butyl-Pyridine as a Probe Molecule to Measure External Acidity of Zeolites', *Journal of Catalysis*, Vol. 179, pp. 451 – 458.

Cripe, TA, Connor, DS, Vinson, PK, Burckett-St Laurent, CTR & Willman, KW (The Procter and Gamble Company) 1999, *Mid-chain branched alkoxylated sulfate surfactants*, US patent 6 008 181.

de Lucas, A, Canizares, P & Duran, A 2001,'Improving deactivation behaviour of HZSM-5 catalysts', *Applied Catalysis A: General*, Vol. 206, pp. 87 - 93.

Ding, W, Meitzner, GD & Iglesia, E 2002,'The Effects of Silanition of External Acid Sites on the Structure and Catalytic Behaviour of Mo/H-MFI', *Journal of Catalysis*, vol. 206, pp. 14 – 22.

Feulmer , GP, Kissin, YV & Payne, WB 1986, 'Gas chromatographic analysis of branched olefins', *Journal of Chromatographic Science*, vol.24, pp. 164 - 168.

Giacobbe, TJ & Ksenic, GA (Mobil Oil Corporation) 1992, *Process for production of biodegradable surfactants and compositions thereof*, US patent 5 112 519.

Giacobbe, TJ & Ksenic, GA (Mobil Oil Corporation) 1993, *Process for production of biodegradable esters*, US patent 5 245 072.

Haag, WO & Chen, NY 1987, *Catalyst design with zeolites*, John Wiley & sons, New York.

Halgeri, AB & Das, J 2002,'Recent advances in selectivation of zeolites for para-substituted aromatics', *Catalysis today*, vol. 73, pp. 65 – 73.

Houston, CA 1998, 'Higher alcohols: Market forecast 2010', Retrieved on 15 July 2005, *http://www.colin-Houston.com/MULTICLIENT_STUDIES*

Hu, Z, Wei, L, Dong, J, Wang, Y, Chen, S & Peng, S 1999,'Modification of the external surface of MFI by a metal surfactant', *Microporous and Mesoporous Materials*, vol. 28, pp. 49 – 55.

Jensen, MC & Culver, GE (The Procter and Gamble Company) 2001, Detergent-making process using a high active surfactant paste containing mid-chain branched surfactants, US patent 6 294 513.

Keim, W, Fleischhauer, J, Hoffmann, E, , Lodewick, R, Meier, U, Paukert, M & Schmitt, G 1979,'Olefin Oligomerisation', *Journal of Molecular Catalysis*, vol.6, pp.79 - 97.

Kim, JH, koma, Y & Niwa, M 1999,'Control of the pore-opening size of HY zeolite by CVD of silicon alkoxide', *Microporous and Mesoporous Materials,* vol. 32, pp. 37 – 44.

Klemm, E, Seitz, M, Scheidat, H & Emig, G 1998,'Conrolling Acidity and Selectivity of HY-Type Zeolites by Silanation', *Journal of Catalysis*, vol. 173, pp. 177 – 186.

Nicolaides, CP & Scurrell, MS 2001, *Supported Catalysts and Their Applications*, Royal Society of Chemistry, UK.

Noweck, K 2002,' Fatty alcohols', in *Ullmanns Encyclopedia of Industrial Chemistry,* Vol. 6.

O'Connor, CT & Kojima, M 1990,'Tailored Alkene oligomerization with ASZM-57 Zeolite', Catalysis Today, Vol. 6, pp. 329 -349.

O'Connor, CT 1997,'Oligomerization and Metathesis', *in Handbook of Heterogeneous Catalysis*, vol. 5, pp. 2380, John Wiles – VCH, Germany.

Page, NM, Young, LB & Blain, DA (Mobil Oil Corporation) 1989, *Olefin oligomerisation with surface modified catalyst*, US patent 4 870 038.

Parenago, OO, Lebedeva, OE, Ivanova, II & Lunina, EV 1993,'Acidity of the external surface of modified pentasil catalysts and its resistance to mechanical treatment', *Pure & Applied Chemistry*, vol. 65, no. 10, pp. 2205 – 2208.

Pater, JPG, Jacobs, PA, & Martens, JA 1999, 'Oligomerisation of hex-1-ene over acidic aluminosilicate zeolites, MSO, and silica-alumina co-gel catalysts: A comparative study', *Journal of Catalysis,* vol. 184, no.1, pp. 262-267.

Quann, RJ, Green, LA, Tabak, SA & Krambeck, FJ 1988, 'Chemistry of olefin oligomerisation over MFI catalyst', *Industrial and Engineering Chemical Research,* vol. 27, pp. 565 - 570

Reklaitis, GV & Schneider, DR 1983, *Introduction to Material and Energy Balances*, John Wiley and Sons, New York.

Roger, HP, CT, Moller, KP & O'Connor 1997,'The transformation of 1,2,4-trimethylbenzene: A probe reaction to monitor external surface modification of H-MFI?, *Microporous Materials*, vol. 8, pp. 151 – 157.

Rosen, MJ 1989,'*Surfactants and Interfacial Phenomena'*, 2nd Ed., John Weley & Sons, USA.

Sakuneka, TM 2004,'Synthesis, characterization and evaluation of an industrially important zeolite of different levels of crystallinity', MSc Thesis, University of the North.

Schick, MJ 1966,'Nonionic Surfactants', *in Surfactant Science Series*, Vol. 1, Marcel Dekker, Inc., New York.

Shaikh, RA, Hegde, SG, Behlekar, AA & Rao, BS 1999,'Enhancement of acidity and paraselectivity by the silanation in pentasil zeolites', *Catalysis Today*, vol. 49, pp. 201 – 209.

Singleton, DM, Kravertz, L, & Murray, BD (Shell Oil Company) 1998a, *Dimerised alcohol compositions and biodegradable surfactants made therefrom having cold water detergency*, US patent 5 780 694.

Singleton, DM, Kravertz, L, & Murray, BD (Shell Oil Company) 1998b, *Highly branched primary alcohol compositions, and biodegradable detergents made therefrom*, US patent 5 849 960.

Singleton, DM, Kravertz, L, & Murray, BD (Shell Oil Company) 2001, *Dimerised alcohol compositions and biodegradable surfactants made therefrom having cold water detergency*, US patent 6 222 077.

Skupińska, J 1991, 'Oligomerisation of α-olefins to higher oligomers', *Chemical Reviews*, vol. 91, pp. 613 - 648.

Stache, HW 1996,'Anionic Surfactants', *in Surfactant Science Series*, Vol.56, Marcel Dekker, Inc., New York.

Stöcker, M 2005, 'Gas phase catalysis by zeolites', *Microporous and Mesoporous Materials*, vol. 82, pp. 257 – 292.

Venuto, PB 1994, 'Organic catalysis over zeolites: a perspective on reaction paths within pores', *Microporous Materials*, vol.2, pp. 297 – 411.

Vinson, PK, Foley, PR, Cripe, TA, Connor, DS & Willman, KW (The Procter and Gamble Company) 2000, *Detergent compositions containing selected mid-chain branched surfactants*, US patent 6 015 781.

Weber, RW, Moller, PK & O'Connor CT 2000,'The chemical vapour and liquid deposition of tetraethoxysilane on MFI, mordenite and beta', *Microporous and Mesoporous Materials,* vol. 35 – 36, pp. 533 – 543.

APPENDIX A

Explanation of data tables

The raw data work-up was according to the equations shown in the data work-up section (4.6.1)

(1) Catalyst pre-treatment conditions were kept the same for all experiments.

(2) Catalysts with an 'e' superscript were in 1/16" extrudate form and those with 'p' were in a powder form.

(3) The conditions shown at the beginning of each table are the set points.

(4) Experiments incorporating co-feed of a nitrogen base, identify the base on the table.

(5) Conversion is that of 1-hexene to products other than C_6s'.

(6) Selectivity is in wt% to dimers.

(7) For extrudates 20% binder was excluded in the determination of space velocity (WHSV)

PRETREATMENT CONDITIONS

Feed	Flowrate (ml/min)	Temperature (°C)	Time (hours)
Pure N_2	50	250	1

EXPERIMENT 1a: Temperature – 160°C, Pressure – 30 bar, WHSV – 2.2 g/g.h, 2.01g MFI-90^{P}

Temperature (°C)	Pressure (bar)	WHSV (g/g.h)	TOS (hours)	Conversion (wt%)	Selectivity (wt%)
160.0	30.1	2.2	7	37.4	76.4
160.0	30.0	2.2.	9	39.7	84.9
160.0	29.9	2.2	10	45.3	73.1
160.0	29.9	2.2	12	45.5	76.4
160.0	29.9	2.2	14	52.1	74.1
160.0	29.8	2.2	17	60.2	671.6
160.0	30.0	2.2	21	64.9	68.0
160.0	30.0	2.2	22	70.4	65.5
160.0	30.1	2.2	23	74.0	65.4
160.0	29.9	2.2	27	82.5	71.6
160.0	29.9	2.2	27	87.1	69.1
160.0	29.9	2.2	28	87.1	66.5
160.0	30.1	2.2	28	88.5	70.3
160.0	30.6	2.2	33	92.6	70.6
160.0	30.0	2.2	38	94.9	73.4
160.0	30.0	2.2	39	95.0	74.7
160.0	29.9	2.2	40	95.4	75.2
160.0	29.8	2.2	41	95.6	76.2
160.0	30.1	2.2	42	95.4	76.6
160.0	30.0	2.2	44	95.5	78.0
160.0	30.0	2.2	45	95.4	77.1
160.0	30..0	2.2	46	95.6	77.2
160.0	30.0	2.2	54	95.1	80.8
160.0	30.0	2.2	65	94.8	83.4

EXPERIMENT 1b: Temperature – 160°C, Pressure – 30 bar, WHSV – 2.2 g/g.h, 2.00g MFI-90^{P}

Temperature (°C)	Pressure (bar)	WHSV (g/g.h)	TOS (hours)	Conversion (wt%)	Selectivity (wt%)
160.0	30.1	2.2	7	44.4	75.7
160.0	30.0	2.2.	8	49.2	75.1
160.0	29.9	2.2	11	63.6	68.6
160.0	29.9	2.2	12	67.5	69.1
160.0	29.9	2.2	18	86.8	68.8
160.0	29.8	2.2	24	90.4	69.8
160.0	30.0	2.2	25	88.6	69.9
160.0	30.0	2.2	26	90.3	71.4
160.0	30.1	2.2	27	90.6	71.3
160.0	29.9	2.2	28	91.2	71.5
160.0	29.9	2.2	30	91.5	73.2
160.0	29.9	2.2	30	92.3	72.2
160.0	30.0	2.2	31	92.5	73.5
160.0	30.1	2.2	33	92.6	74.3
160.0	30.0	2.2	34	93.1	74.0
160.0	30.0	2.2	41	93.3	75.0
160.0	30.1	2.2	48	93.2	76.7
160.0	29.9	2.2	49	93.0	77.3
160.0	30.1	2.2	50	92.9	77.6
160.0	30.0	2.2	53	92.6	76.8
160.0	30.0	2.2	55	92.2	79.0

EXPERIMENT 1c: Temperature – 160°C, Pressure – 30 bar, WHSV – 2.2 g/g.h, 2.03g MFI-90^{p}

Temperature (°C)	Pressure (bar)	WHSV (g/g.h)	TOS (hours)	Conversion (wt%)	Selectivity (wt%)
160.0	29.9	2.2	9	69.1	79.3
160.0	29.9	2.2	19	84.6	78.4
160.0	30.0	2.2	20	89.4	78.2
160.0	30.1	2.2	22	92.4	78.7
160.0	30.0	2.2	26	93.9	80.1
160.0	30.0	2.2	34	94.4	82.3
160.0	30.1	2.2	42	93.8	83.5
160.0	30.1	2.2	45	93.9	83.7

EXPERIMENT 2: Temperature – 160°C, Pressure –30 bar, WHSV – 4.4 g/g.h, 2.01g MFI-90^{p}

Temperature (°C)	Pressure (bar)	WHSV (g/g.h)	TOS (hours)	Conversion (wt%)	Selectivity (wt%)
159.8	29.8	4.4	7	56.8	85.6
160.0	29.9	4.4	15	66.0	80.7
160.0	30.1	4.4	16	66.6	80.9
160.0	30.0	4.4	18	66.4	81.5
160.0	30.0	4.4	20	63.7	81.9
159.9	30.0	4.4	22	61.7	83.6
160.0	29.9	4.4	25	59.8	85.4
160.0	30.0	4.4	33	53.3	88.2

EXPERIMENT 3: Temperature – 160°C, Pressure – 30 bar, WHSV – 6.6 g/g.h, 2.02g MFI-90^{p}

Temperature (°C)	Pressure (bar)	WHSV (g/g.h)	TOS (hours)	Conversion (wt%)	Selectivity (wt%)
160.0	29.8	6.6	8	18.5	96.4
160.0	30.0	6.6	9	22.4	96.7
160.0	30.0	6.6	10	29.4	96.7
160.0	30.1	6.6	11	32.3	97.7
160.0	29.9	6.6	12	30.3	97.5
160.0	29.9	6.6	12	33.3	93.8
160.0	29.9	6.6	15	31.6	89.2
160.0	30.0	6.6	16	32.0	81.6
160.0	30.1	6.6	17	37.6	82.8
160.0	30.0	6.6	21	36.2	90.9
160.0	30.0	6.6	27	38.8	80.5
160.0	30.1	6.6	30	40.3	79.4

EXPERIMENT 4: Temperature – 160°C, Pressure – 30 bar, WHSV – 1.1 g/g.h, 2.00g MFI-120^{p}

Temperature (°C)	Pressure (bar)	WHSV (g/g.h)	TOS (hours)	Conversion (wt%)	Selectivity (wt%)
160.0	30.1	1.1	8	18.2	92.2
160.0	29.9	1.1	11	19.1	94.8
160.0	29.9	1.1	12	17.2	95.5
160.0	29.9	1.1	23	20.1	95.3
160.0	30.0	1.1	23	24.1	94.3
160.0	30.1	1.1	24	27.2	94.3

EXPERIMENT 5: Temperature – 160°C, Pressure – 30 bar, WHSV – 2.2 g/g.h, 2.00g MFI-220[P]

Temperature (°C)	Pressure (bar)	WHSV (g/g.h)	TOS (hours)	Conversion (wt%)	Selectivity (wt%)
160.0	30.0	2.2	12	1.2	93.9
160.0	30.1	2.2	13	1.7	100.0
160.0	29.9	2.2	14	2.4	100.0
160.0	29.9	2.2	16	3.0	100.0
160.0	29.9	2.2	18	2.9	100.0
160.0	30.0	2.2	20	2.5	100.0

EXPERIMENT 6: Temperature – 160°C, Pressure – 30 bar, WHSV – 2.2 g/g.h, 2.00g MFI-400[P]

Temperature (°C)	Pressure (bar)	WHSV (g/g.h)	TOS (hours)	Conversion (wt%)	Selectivity (wt%)
160.0	30.0	2.2	1	3.6	99.2
160.0	30.1	2.2	2	2.1	99.7
160.0	30.0	2.2	5	1.3	100.0
160.0	30.0	2.2	7	1.0	98.3
160.0	30.0	2.2	8	0.8	100.0

EXPERIMENT 7: Temperature – 160°C, Pressure – 30 bar, WHSV – 2.2 g/g.h, 2.01g MFI-90[P]

Temperature (°C)	Pressure (bar)	WHSV (g/g.h)	TOS (hours)	Conversion (wt%)	Selectivity (wt%)
160.0	30.0	2.2	7	44.4	75.7
160.0	30.1	2.2	8	49.2	75.1
160.0	29.9	2.2	11	63.6	68.6
160.0	29.9	2.2	12	67.5	69.1
160.0	29.9	2.2	18	86.8	68.8
160.0	30.0	2.2	24	90.4	69.8
160.0	30.1	2.2	25	88.6	69.9
160.0	30.0	2.2	26	90.3	71.4
160.0	30.0	2.2	27	90.6	71.3
160.0	30.1	2.2	28	91.2	71.5
160.0	29.9	2.2	30	91.5	73.2
160.0	30.1	2.2	30	92.3	72.2
160.0	30.0	2.2	31	92.5	73.5
160.0	30.0	2.2	33	92.6	74.3
160.0	30..0	2.2	34	93.1	74.0

EXPERIMENT 8: Temperature – 160°C, Pressure –30 bar, WHSV – 2.2 g/g.h, 2.02g BEA-150[P]

Temperature (°C)	Pressure (bar)	WHSV (g/g.h)	TOS (hours)	Conversion (wt%)	Selectivity (wt%)
160.0	30.0	2.2	3	9.0	81.6
160.0	30.1	2.2	4	10.0	77.7
160.0	30.0	2.2	20	50.0	79.9
160.0	30.0	2.2	22	50.7	80.4
160.0	30.1	2.2	24	48.6	81.3
160.0	29.9	2.2	27	46.7	82.4
160.0	30.1	2.2	34	40.4	84.4
160.0	30.0	2.2	45	34.4	88.0
160.0	30.0	2.2	46	34.8	87.4
160.0	30..0	2.2	50	32.4	88.5
160.0	29.9	2.2	58	26.9	89.9

EXPERIMENT 9: Temperature – 160°C, Pressure –30 bar, WHSV – 4.4 g/g.h, 2.01g TON-90[p]

Temperature (°C)	Pressure (bar)	WHSV (g/g.h)	TOS (hours)	Conversion (wt%)	Selectivity (wt%)
160.0	30.0	4.4	2	13.2	81.5
160.0	30.1	4.4	3	18.9	80.9
160.0	30.0	4.4	18	47.6	86.0
160.0	30.0	4.4	20	47.3	86.3
160.0	30.1	4.4	23	46.5	83.9
160.0	29.9	4.4	25	44.1	83.6
160.0	30.1	4.4	28	44.0	85.7
160.0	30.0	4.4	45	34.6	88.0

EXPERIMENT 10: Temperature – 160°C, Pressure – 30 bar, WHSV – 4.4 g/g.h, 2.00g SA[p]

Temperature (°C)	Pressure (bar)	WHSV (g/g.h)	TOS (hours)	Conversion (wt%)	Selectivity (wt%)
160.0	30.0	4.4	2	10.6	83.4
160.0	30.0	4.4	8	52.3	71.9
159.9	30.0	4.4	9	64.8	72.6
160.0	30.0	4.4	19	69.6	71.3
160.0	30.1	4.4	19	68.2	72.7
160.0	30.0	4.4	20	70.2	71.7
159.8	30.0	4.4	23	69.9	71.5
160.0	30.1	4.4	26	68.9	72.6
160.0	29.9	4.4	34	66.4	73.8
160.0	30.1	4.4	43	62.0	76.9
159.9	30.0	4.4	45	61.7	78.0
160.0	30.0	4.4	47	61.5	77.3
160.0	30..0	4.4	50	59.5	77.8
160.0	30.0	4.4	51	58.9	77.8
160.0	30.1	4.4	59	56.7	79.1
160.0	30.0	4.4	68	55.8	78.9

EXPERIMENT 11: Temperature – 170°C, Pressure – 20 bar, WHSV – 1.1 g/g.h, 5.7g MFI-90[e]

Temperature (°C)	Pressure (bar)	WHSV (g/g.h)	TOS (hours)	Conversion (wt%)	Selectivity (wt%)
170.0	20.1	1.1	3	17.2	97.4
170.0	20.0	1.1	14	67.4	73.4
170.0	19.9	1.1	25	81.8	76.2
170.0	20.0	1.1	45	83.8	81.2
170.0	19.9	1.1	66	78.9	84.0
170.0	19.8	1.1	67	77.2	85.5
170.0	20.0	1.1	68	77.9	84.8
170.0	20.0	1.1	70	77.5	85.1
170.0	20.0	1.1	72	77.6	84.7
170.0	19.9	1.1	80	74.8	85.5

EXPERIMENT 12: Temperature – 170°C, Pressure – 40 bar, WHSV – 1.1 g/g.h, 5.71g MFI-90[e]

Temperature (°C)	Pressure (bar)	WHSV (g/g.h)	TOS (hours)	Conversion (wt%)	Selectivity (wt%)
170.0	40.1	1.1	8	44.5	78.1
170.0	40.0	1.1	17	78.2	75.1
170.0	40.9	1.1	19	84.3	75.7
170.0	40.0	1.1	21	84.3	77.0
170.0	40.9	1.1	23	85.0	76.3
170.0	40.8	1.1	25	82.4	78.6
170.0	40.0	1.1	33	77.8	77.1
170.0	40.0	1.1	41	78.8	77.2
170.0	40.0	1.1	51	80.1	79.4
170.0	40.9	1.1	52	79.7	80.1
170.0	40.9	1.1	59	79.0	78.9
170.0	40.9	1.1	70	77.3	78.9
170.0	40.1	1.1	81	76.9	79.8
170.0	40.6	1.1	93	76.6	79.5

EXPERIMENT 13: Temperature – 160°C, Pressure – 30 bar, WHSV – 1.1 g/g.h, 5.70g MFI-90[e]

Temperature (°C)	Pressure (bar)	WHSV (g/g.h)	TOS (hours)	Conversion (wt%)	Selectivity (wt%)
160.0	30.0	1.1	7	51.3	81.8
160.0	30.0	1.1	15	76.5	81.0
160.0	30.1	1.1	16	85.3	79.3
160.0	30.0	1.1	18	87.6	80.0
160.0	30.0	1.1	20	87.3	82.2
160.0	30.1	1.1	22	86.1	83.4
160.0	29.9	1.1	30	78.6	86.4
160.0	30.1	1.1	39	74.2	87.7
160.0	30.0	1.1	42	71.9	89.5
160.0	30.0	1.1	55	64.8	90.9
160.0	30..0	1.1	66	60.5	91.7
160.0	30.0	1.1	77	48.1	93.0
160.0	30.1	1.1	89	38.2	94.3

EXPERIMENT 14:; Temperature – 150°C, Pressure – 20 bar, WHSV – 1.1 g/g.h, 5.70g MFI 90[e]

Temperature (°C)	Pressure (bar)	WHSV (g/g.h)	TOS (hours)	Conversion (wt%)	Selectivity (wt%)
150.0	20.0	1.1	7	30.8	90.2
150.0	19.9	1.1	15	43.6	90.3
150.0	20.0	1.1	16	53.1	90.4
150.0	19.9	1.1	18	55.5	91.8
150.0	19.8	1.1	19	51.9	91.5
150.0	20.0	1.1	21	48.2	92.6
150.0	20.0	1.1	24	44.6	92.3
150.0	20.0	1.1	31	38.5	94.6
150.0	19.9	1.1	39	35.6	95.1
150.0	20.0	1.1	41	33.5	94.8
150.0	19.9	1.1	44	30.8	94.9
150.0	20.0	1.1	54	26.8	95.9
150.0	19.9	1.1	63	23.5	94.9
150.0	19.9	1.1	65	23.4	96.2
150.0	20.0	1.1	67	22.5	96.2
150.0	20.0	1.1	70	21.5	96.3

EXPERIMENT 15: Temperature – 150°C, Pressure – 40 bar, WHSV – 1.1 g/g.h, 5.72g MFI 90[e]

Temperature (°C)	Pressure (bar)	WHSV (g/g.h)	TOS (hours)	Conversion (wt%)	Selectivity (wt%)
150.0	40.1	1.1	8	39.8	89.2
150.0	40.0	1.1	16	59.8	92.8
150.0	40.4	1.1	18	74.9	83.3
150.0	40.0	1.1	19	77.5	84.1
150.0	40.1	1.1	21	79.1	85.3
150.0	40.1	1.1	23	80.4	86.5
150.0	40.0	1.1	31	71.8	90.0
150.0	40.0	1.1	39	69.7	91.0
150.0	40.0	1.1	42	64.5	92.0
150.0	40.1	1.1	44	64.2	93.1
150.0	40.0	1.1	53	51.4	94.9
150.0	39.9	1.1	63	49.5	94.9
150.0	40.0	1.1	66	46.5	94.5

EXPERIMENT 16: Temperature – 170°C, Pressure – 20 bar, WHSV – 1.1 g/g.h, 5.71g MFI 90[e], 65 ppm 2,4,6-Collidine

Temperature (°C)	Pressure (bar)	WHSV (g/g.h)	TOS (hours)	Conversion (wt%)	Selectivity (wt%)
170.0	19.9	1.1	8	54.9	79.9
170.0	20.0	1.1	16	68.0	77.8
170.0	19.8	1.1	21	72.2	78.8
170.0	20.0	1.1	23	79.4	76.9
170.0	19.9	1.1	32	89.5	76.2
170.0	20.0	1.1	40	89.5	79.0
170.0	19.8	1.1	43	88.5	81.0
170.0	20.0	1.1	49	78.0	85.8
170.0	19.9	1.1	56	24.1	91.0
170.0	20.0	1.1	64	14.7	92.2
170.0	19.9	1.1	69	8.5	100.0
170.0	20.0	1.1	79	11.0	93.3
170.0	19.9	1.1	88	13.2	90.9
170.0	20.0	1.1	89	12.3	90.0

EXPERIMENT 17: Temperature – 170°C, Pressure – 20 bar, WHSV – 1.1 g/g.h, 5.71g MFI 90[e], 65 ppm 2,6-t-butylpyridine

Temperature (°C)	Pressure (bar)	WHSV (g/g.h)	TOS (hours)	Conversion (wt%)	Selectivity (wt%)
170.0	20.0	1.1	8	54.9	79.9
169.9	20.0	1.1	16	80.3	78.8
170.0	20.0	1.1	17	85.5	79.5
170.0	19.9	1.1	19	87.2	79.3
170.0	20.0	1.1	21	87.8	79.6
170.0	19.9	1.1	23	87.4	80.0
169.8	20.0	1.1	25	86.6	80.6
170.0	20.0	1.1	41	83.5	82.2
170.0	20.0	1.1	64	15.8	90.6
170.0	20.0	1.1	87	4.9	100.0

EXPERIMENT 18: Temperature – 170°C, Pressure – 20 bar, WHSV – 1.1 g/g.h, 5.70g MFI 90[e], 65 ppm 4-Methylquinoline

Temperature (°C)	Pressure (bar)	WHSV (g/g.h)	TOS (hours)	Conversion (wt%)	Selectivity (wt%)
170.0	20.0	1.1	9	76.0	79.3
170.0	20.0	1.1	19	84.4	79.8
170.0	20.0	1.1	21	85.3	81.4
170.0	20.0	1.1	23	85.9	80.7
169.8	20.0	1.1	26	84.9	83.2
170.0	20.0	1.1	33	72.3	88.4
170.0	20.0	1.1	42	68.8	89.6
170.0	20.0	1.1	66	36.4	94.2

APPENDIX B

1-Hexene phase diagram

The phase diagram was drawn by making use of the Antoine Equation in Reklaitis (1983)

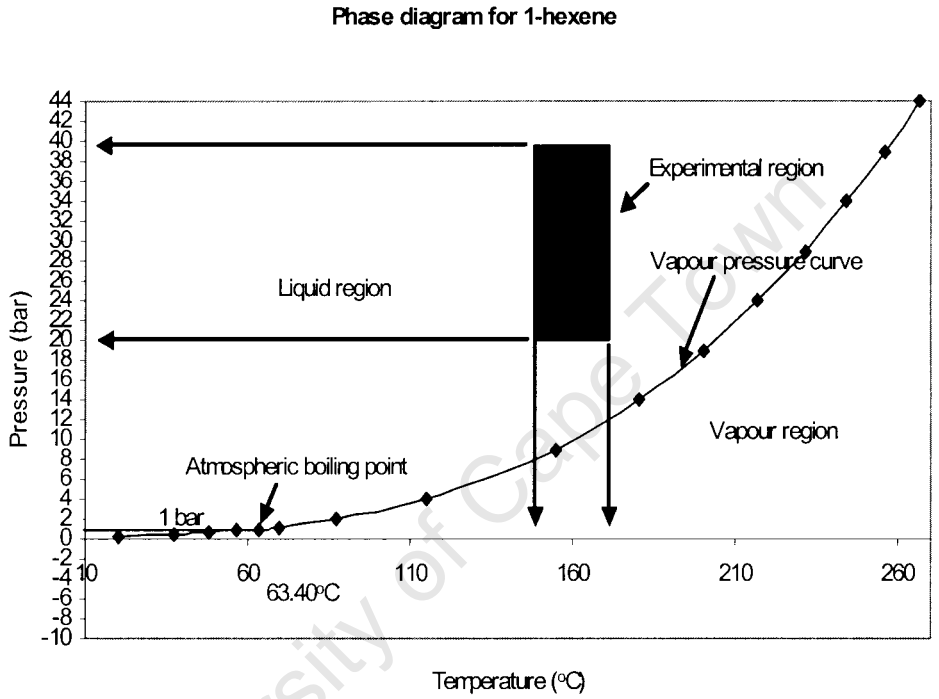

APPENDIX C

Gaspe NMR analyses

The principle of GASPE (C1) is as follows;

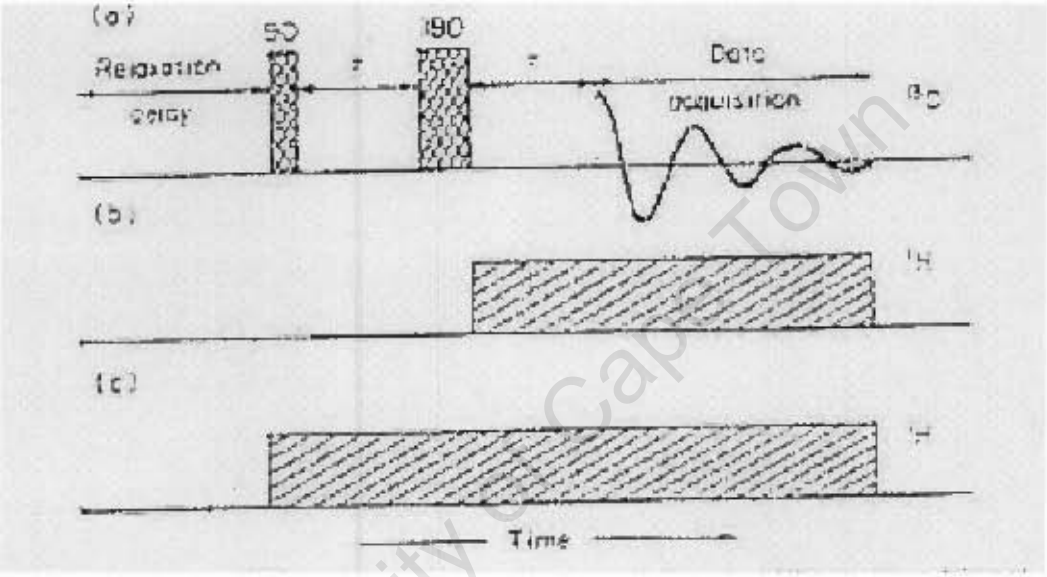

C1: ^{13}C spin echo pulse sequence. When combined with broad band ^{1}H decoupling in the manner shown in (b), or in the manner shown in (c), this yields a gated spin echo (GASPE) sequence. These diagrams are illustrative, and are not drawn to scale (Cookson, 1981).

The ^{13}C portion of the sequence (C1a) is the simple spin-echo procedure; relaxation delay (90 – r – 180 – r) data acquisition. This would result in the formation of an echo after the period 2r. The magnitude of the echo magnetization would be given to a good approximation by

$M_{2r} = M_o e^{-2r/T_2}$, where, M_o is the equilibrium magnetization and T_2 the transverse relaxation time. The ^{1}H portion (C1b) the sequence broad band ^{1}H irradiation is gated on, coincident with the 180 ^{13}C pulse. This causes J modulation of the echo magnitude, in a manner which can be used to identify resonance multiplicity. In this method (GASPE), the

magnitude of the echo magnetization for C, CH, CH_2 and CH_3 are given by the following equations;

C: $M_{2r} = M_0 e^{-2r/T_2}$ 1

CH: $M_{2r} = M_0 e^{-2r/T_2} \cos \pi rJ$ 2

CH_2: $M_{2r} = 0.5 M_0 e^{-2r/T_2}(1 + \cos 2\pi rJ)$ 3

CH_3: $M_{2r} = 0.75 M_0 e^{-2r/T_2}(\cos \pi rJ + 0.3 \cos 3\pi rJ)$ 4

In all cases the exponential factor e^{-2r/T_2} denotes transverse relaxation during the period 2r. If $2r << T_2$, then this factor approximates unity and the curves in C2 show the echo J modulation as a fuction of time. The distinctive behaviour of C, CH, CH_2 and CH_3 carbon resonances shown in C2 forms the basis of the assignment of resonance multiplicity in the present work.

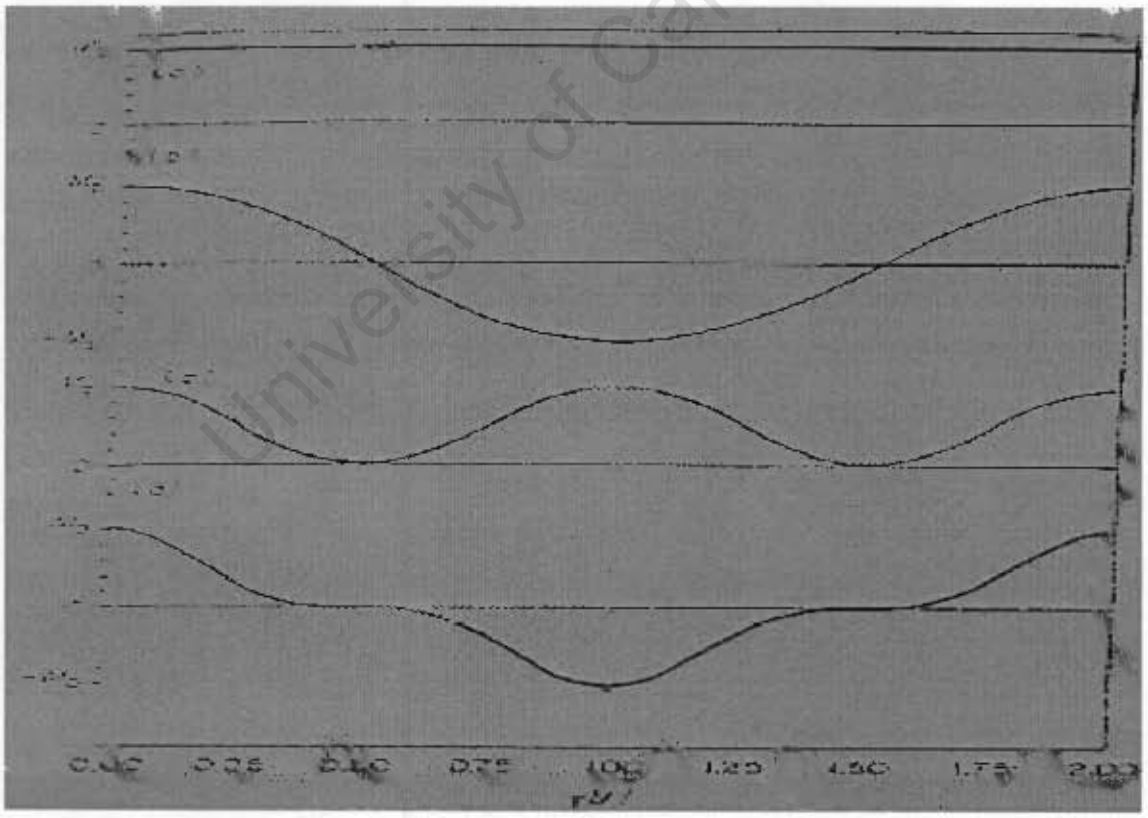

C2: J modulation of the echo magnitude for multiplets, (a) C, (b) CH, (c) CH_2 and (d) CH_3, using the GASPE sequence illustrated in C1. The curves are derived from the equations 1 – 4.

The above-mentioned method was incorporated into the NMR instrument in order to determine the branching on the C_{12} fractions from the dimerization reactions. The program is as given below. The information on typical spectra obtainable and a list of possible structures identified is also provided.

```
"gaspeproc"  "Copyright Megan Kirk, Sasol Technology"
'Gaspe Processing.  THis macro takesthe 5 gaspe spectra and uses them to produ

aig='ai'
cutoff=25
jexp:$curexp


"CH'S"
clradd
select(1) add( 1.4142)
select(3) add(-1.4142)
select(5) add(-0.5)
select(4) add( 0.5)

svtmp('gaspe')
mf(5,$curexp)
svtmp('ch') rttmp('gaspe')

"CH2's"
clradd
select(5) add( 0.5)
select(4) add( 0.5)
select(2) add(-1)

svtmp('gaspe')
mf(5,$curexp)
svtmp('ch2') rttmp('gaspe')

"CH3's"
clradd
select(5) add
select(4) add(-1)
select(1) add(-1.4142)
select(3) add( 1.4142)

svtmp('gaspe')
mf(5,$curexp)
svtmp('ch3') rttmp('gaspe')

"CH + CH3"
clradd
ds(5) add(0.5)
ds(4) add(-0.5)
svtmp('gaspe')
mf(5,$curexp)
svtmp('ch3+ch') rttmp('gaspe')

"C's"
clradd
select(2) add

"Copy all to exp 5"
mt($curexp,5)
rttmp('ch') wft select add('new')
rttmp('ch2') wft select add('new')
rttmp('ch3') wft select add('new')
rttmp('ch3+ch') wft select add('new')
rttmp('gaspe')
```

```
"move processed spectra back to current exp"

rf(5,$curexp)
wft
svtmp('proc')
rttmp('proc')

"dc baseline corrections"

select(1) dc bc
select(2) dc bc
select(3) dc bc
select(4) dc bc
select(5) dc bc

gaspecalmp2

ins?

gaspedisplay
```

Typical spectra for different products obtained during the dimerization of 1-hexene over various catalysts (Bekker, 2003) are shown below;.

MFI-90 catalysed hydrogenated C_{12} fraction

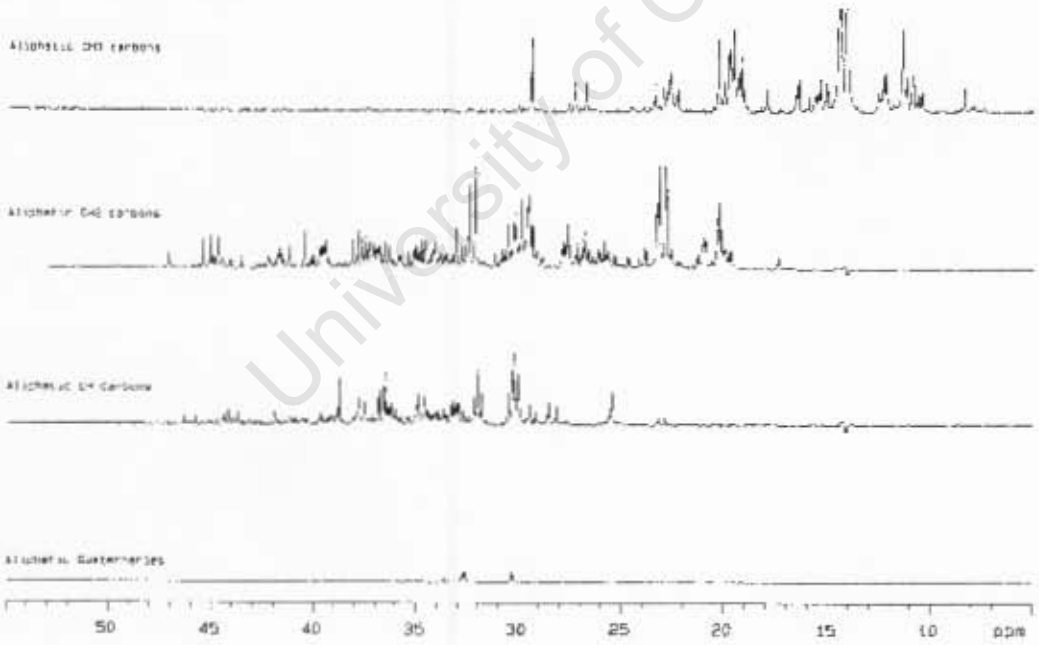

Siral-40 catalysed hydrogenated C_{12} fraction

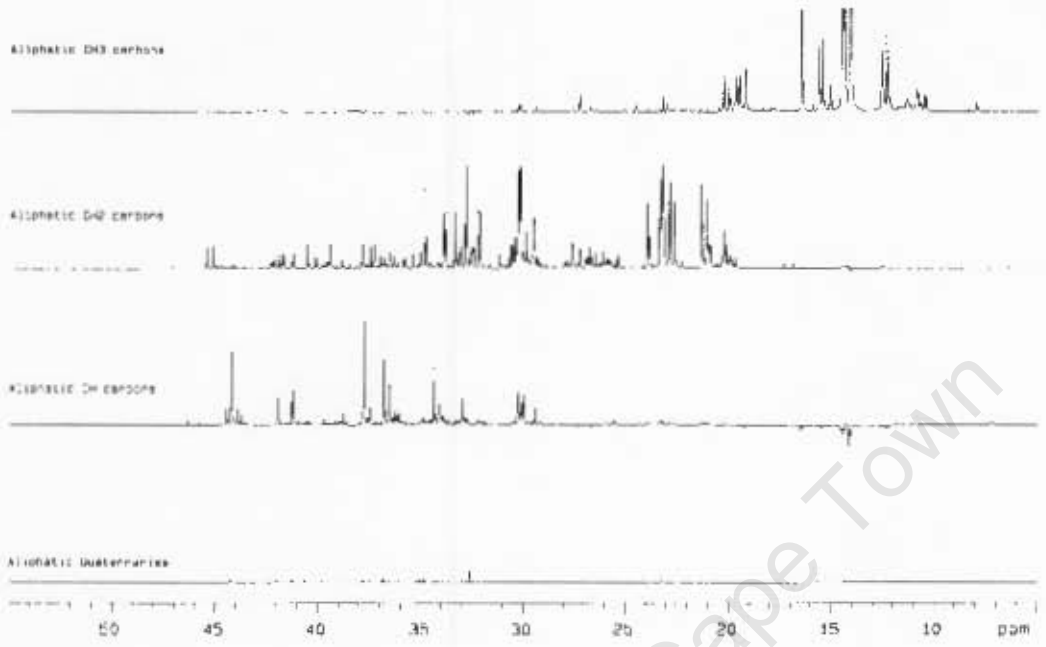

TON-90 catalysed hydrogenated C_{12} fraction

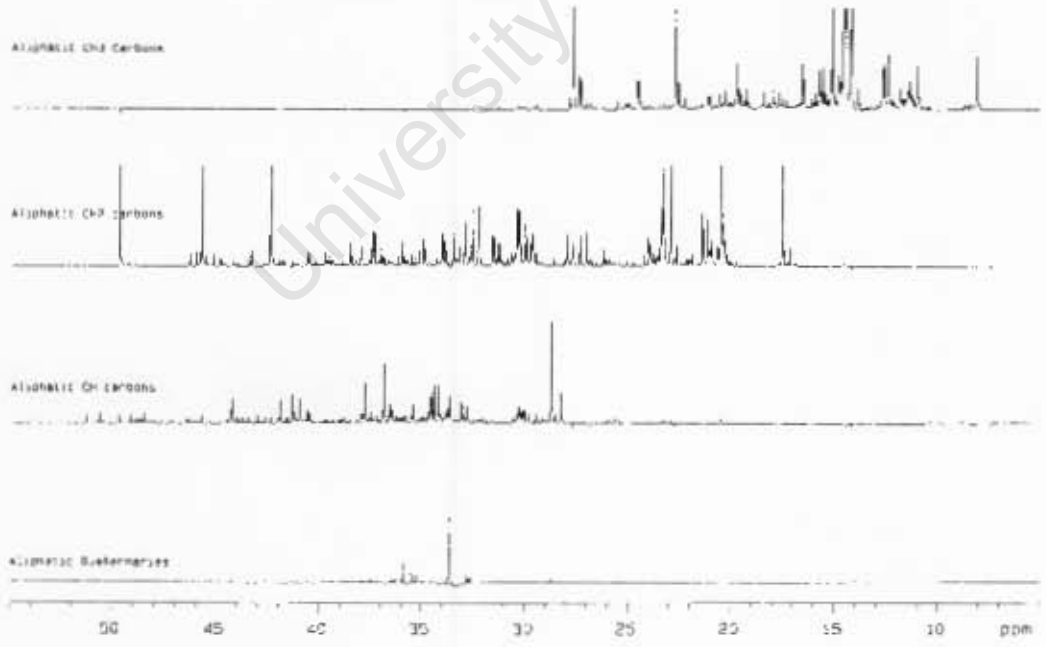

BEA-150 catalysed hydrogenated C_{12} fraction

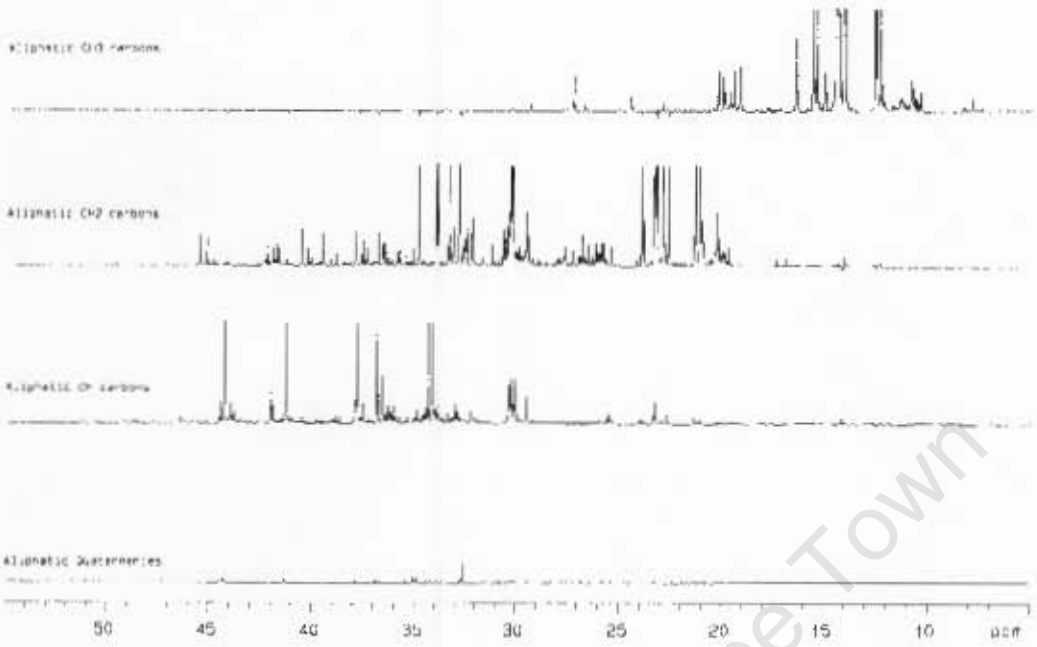

Possible structures that could be obtained when 1-hexene is dimerised over acid catalysts (Bekker, 2003).

1A

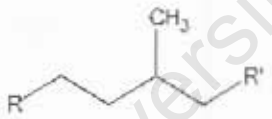

1B

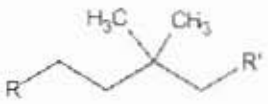

1C

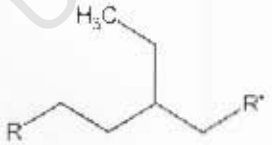

1D

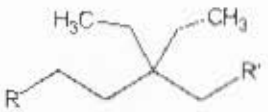

1E

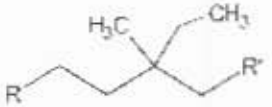

1F

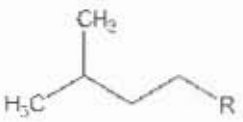

Generic structures for possible branching for 1 branch site

2A 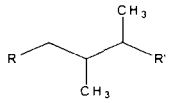

2B 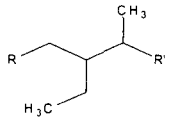

2C 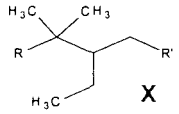
X

2D 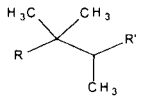

2F 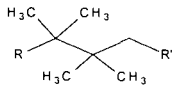

2E 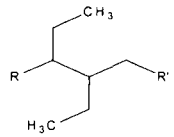

2G 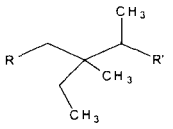

2H 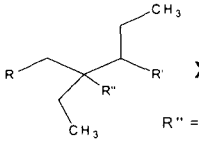
X

R'' = Me or Et

2I 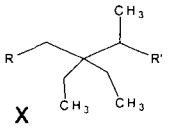
X

2J 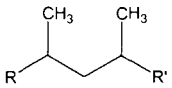

2K 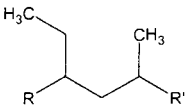

2L 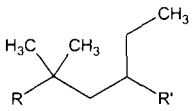

2M 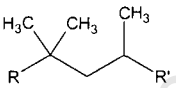

2N 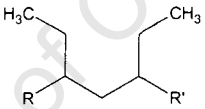

2O 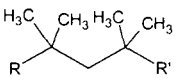

2P 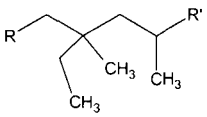

2Q 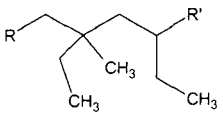

2R 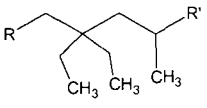

Generic Structures for possible branching for 2 branch sites

3A 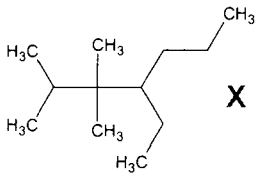 X

3B 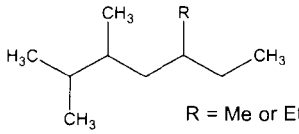 R = Me or Et

3C 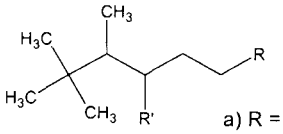 a) R = Me, R' = Et
b) R = Et, R' = Me

3D 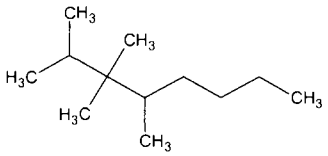

3E 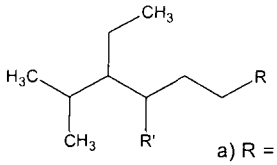 a) R = Me, R' = Et
b) R = Et, R' = Me

3F 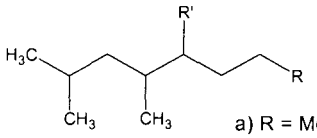 a) R = Me, R' = Et
b) R = Et, R' = Me

Generic Structures for possible branching for 3 branch sites (assuming no rearrangement after coupling)